



Samuel Ramos Pereira
BSc in Biotechnology

Variation of venom composition and toxicity in weever fishes (Trachinidae). Implications for biomedicine and biotechnology.

MASTER IN MOLECULAR GENETICS AND BIOMEDICINE
NOVA University Lisbon
September, 2024



NOVA

NOVA SCHOOL OF
SCIENCE & TECHNOLOGY

DEPARTMENT OF LIFE SCIENCES

Variation of venom composition and toxicity in weever fishes (Trachinidae). Implications for biomedicine and biotechnology.

Samuel Ramos Pereira

BSc in Biotechnology

Adviser: Pedro M. Costa
Auxiliary Professor, NOVA University Lisbon

Co-adviser: Carolina Madeira
Researcher, NOVA University Lisbon

Examination Committee:

Chair: Ana Rita Fialho Grosso
Assistant Professor, NOVA University of Lisbon

Rapporteur: Tiago Fernandes Grilo
Auxiliary Professor, Faculty of Sciences, University of Lisbon

Adviser: Pedro M. Costa
Auxiliary Professor, NOVA University Lisbon

MASTER IN Molecular Genetics and Biomedicine

NOVA University Lisbon

September, 2024

Variation of venom composition and toxicity in weever fishes (Trachinidae). Implications for biomedicine and biotechnology.

Copyright © Samuel Ramos Pereira, NOVA School of Science and Technology, NOVA University Lisbon.

The NOVA School of Science and Technology and the NOVA University Lisbon have the right, perpetual and without geographical boundaries, to file and publish this dissertation through printed copies reproduced on paper or on digital form, or by any other means known or that may be invented, and to disseminate through scientific repositories and admit its copying and distribution for non-commercial, educational or research purposes, as long as credit is given to the author and editor.

ACKNOWLEDGMENTS

I want to start by thanking my adviser, professor Pedro Costa and my co-adviser, professor Carolina Madeira for this great opportunity of working with them as well as the patience they had with me and all their help during this long phase of my studies.

I also want to give a special thanks to all the SeaTox lab members that helped me during all the work done both inside and outside the laboratory. Specially Inês Cabral, Inês Padrão, Carla Martins, Catarina Faustino and Ana Rodrigo for all the help and advice they gave me.

I would like to thank all my friends that like me went to the making of their thesis project facing the same struggles. During this time talking with them always helped me feel better, especially their kind words and all their good advice, as well as the fun times we shared during these years of our master's degree.

My family members too were a great help during this time helping me with great encouragement and all their advice not only for this thesis but also for my future challenges.

Last but not least I would like to thank from the bottom of my heart my life partner Matilde Pires for all the help she gave during this last five years of mine. During this time a lot of events happened. Some really good, others not so much. But she always stayed by my side during every single one of them. She had always the right words of encouragement for me when times were rough, and it is due to her help that I can continue to move on in life and accept all the challenges that have yet to come.

"Yesterday is history, tomorrow is a mystery, today is a gift of God, which is why we call it the present." (Bill Keane).

ABSTRACT

Blue Biotechnology, also known as marine biotechnology, is a specialized area within biotechnology that focuses on the exploration and exploitation of marine resources to develop new products and technologies, that eventually can be used and applied in a variety of different areas reaching from pharmaceuticals and personal care products to aquaculture. Despite the interest on venoms for drug discovery, only recently have fish venoms caught the attention of biotechnologists. Indeed, only a few species have so far been studied in detail. One of those species native to our homeland coast is the lesser weever fish (*Echiichthys vipera*) which is responsible for one of the most painful stings from all animal kingdom. This thesis aims to contribute to the investigation of the main venom apparatus of the weever fish, where venom production takes place and the way envenomation occurs, as well as identify the most important proteinaceous toxins present in weever fish venom as well as locate, isolate, sequence and quantitate the expression levels mRNAs coding for these toxins per sex of fish. Histology revealed the morphology of the venom glands responsible for venom production in both dorsal and opercular spines. In addition, two proteinaceous toxins present in the venom were identified, an alfa and a beta subunit of a cytolytic pore-forming toxin also known as cytolysin. Quantitative RT-PCR analysis showed that there was a significant increase in the expression of those subunits in the venomous dorsal and opercular spines compared to the soft rays, but there was no evidence found for a difference in expression between males and females.

Keywords: Lesser weever fish, Blue Biotechnology, Cytolysin, Venom, Gene expression

RESUMO

A Biotecnologia Azul, também conhecida como biotecnologia marinha, é uma área especializada dentro da biotecnologia que se concentra na exploração e aproveitamento de recursos marinhos para desenvolver novos produtos e tecnologias, que eventualmente podem ser usados e aplicados em uma variedade de áreas diferentes, atingindo desde produtos farmacêuticos e produtos de higiene pessoal até a aquicultura. Apesar do interesse nos venenos para a descoberta de medicamentos, só recentemente os venenos de peixes chamaram a atenção dos biotecnólogos. Na verdade, apenas algumas espécies foram até agora estudadas em detalhe. Uma dessas espécies nativas da costa da nossa terra natal é o peixe-aranha (*Echiichthys vipera*), responsável por uma das picadas mais dolorosas de todo o reino animal. Esta tese visa contribuir para a investigação do principal aparelho venenoso do peixe-aranha, onde ocorre a produção de veneno e a forma como ocorre o envenenamento, bem como identificar as toxinas proteicas mais importantes presentes no veneno do peixe-aranha, tal como localizar, isolar, sequenciar e quantificar os níveis de expressão de mRNAs que codificam essas toxinas por sexo dos peixes. A histologia revelou a morfologia das glândulas de veneno responsáveis pela produção de veneno nas espinhas dorsal e opercular. Além disso, foram identificadas duas toxinas proteicas presentes no veneno, uma subunidade alfa e uma subunidade beta de uma toxina citolítica formadora de poros, também conhecida como citolisina. A análise quantitativa por RT-PCR mostrou que houve um aumento significativo na expressão dessas subunidades nos espinhos venenosos dorsais e operculares em comparação com os raios moles, mas não foram encontradas evidências da diferença na expressão entre machos e fêmeas.

Palavras-chave: Peixe-aranha, Biotecnologia Azul, Citolisina, Veneno, Expressão genética

CONTENTS

1	INTRODUCTION	1
1.1	Ocean biodiversity and bioprospecting for novel bioactives: past trends and future challenges	1
1.2	Venomous animals: physiology, ecology and evolution.....	2
1.3	Marine toxins as highly prized bioproducts: applications and opportunities.	6
1.4	Weever fishes: marine vertebrates with potential for toxin biodiscovery, mechanistic insights and research translation.....	7
1.5	Thesis objectives and hypothesis	8
1.6	Thesis relevance to science and society	9
2	MATERIALS AND METHODS	11
2.1	Animals and Sampling	11
2.2	Histology	12
2.3	RNA Extraction	13
2.4	Reverse transcription of RNA to cDNA	13
2.5	Primer Design and Testing	14
2.6	Gene Expression Analyses	16
2.7	Statistical Analysis	16
2.8	Protein Functional analysis	16
2.9	Phylogenetic Analysis	16

3	RESULTS.....	19
3.1	Histology	19
3.2	Toxin subunit alfa and beta Sequence Isolation	22
3.3	Tx A and Tx B Gene Expression.....	24
3.4	Protein Functional Analysis	26
3.5	Phylogeny	26
4	DISCUSSION	29
5	CONCLUSIONS AND FUTURE PERSPECTIVES	33
6	REFERENCES.....	35

LIST OF FIGURES

Figure 1.1 Taxonomic diversity and the main primary functions of venom.....	4
Figure 1.2 A phylogenetic tree showing the known clades of venomous fish.....	5
Figure 1.3 Lesser weever (<i>Echiichthys vipera</i>)	8
Figure 2.1 Map of the sampling area	12
Figure 3.1 Histological images from dorsal and opercular venomous spines and dorsal soft-rays from weever fish <i>Echiichthys vipera</i>	21
Figure 3.2 Histological image from opercular venomous spine from weever fish <i>Echiichthys vipera</i>	22
Figure 3.3 Agarose gel electrophoresis of PCR amplified products using cytolysin beta like subunit PCR primers.....	23
Figure 3.4 Agarose gel electrophoresis of PCR amplified products using qRT-PCR primers.....	24
Figure 3.5 Results from all the metrics obtained by qPCR.....	25
Figure 3.6 Maximum log-likelihood phylogenetic tree	27

LIST OF TABLES

Table 2.1 Relevant genes for qPCR tags Accession List	14
Table 2.2 Relevant genes for PCR primers used in this paper and their respective sequences, annealing temperature and product sizes.	15
Table 2.3 Tx A/Tx B protein sequences Accession List.....	17

INTRODUCTION

1.1 Ocean biodiversity and bioprospecting for novel bioactives: past trends and future challenges

Oceans cover around 71% of our planet's surface and are home to a vast array of biodiversity, with countless species of plants, animals and microorganisms inhabiting its diverse ecosystems. For us humans, these marine environments provide a wide range of services and activities leading to societal and economic benefits, such as fishing, aquaculture and recreational diving (Rotter et al., 2021).

Nowadays new ways of exploring marine resources and the ocean's untapped potential of the unexplored marine life for biologically relevant molecules have become a lot more popular. Marine bioprospecting, for instance, is a fairly new activity which aims for the exploration of the available marine biodiversity for commercially valuable bioactives and genetic resources, or the gathering of information derived from biota, regarding molecular composition of live resources for the development of new natural products (Bekiari, 2023). The chemical diversity and bioactive properties of these molecules allow them to be applied in a wide range of industrial sectors such as blue biotechnologies, cosmetics, and biomedicine (Wan, M. et al., 2021).

Despite marine bioprospecting being such a promising activity, it is also highly controversial. The low concentrations of the biomolecules of interest (from both marine vertebrates and invertebrates) for providing a sustainable supply for pre-clinical and clinical trials is definitely a throwback, that said, chemical characterization and preliminary activity evaluation is still possible and an important step forward, leading us to believe in a significant growth in the next few decades, offering vast research opportunities as well as potential economic and commercial profits (Montaser, 2011). Particularly, the presence of varied biomolecules (e.g. secondary metabolites, enzymes, and others) which have evolved in highly diverse, sometimes extreme environments, to improve the organisms' survival performance in their habitats is one of the most stimulating reasons for pursuing marine bioprospecting and natural product

screening and research. Studies from the past years have shown that marine biomolecules can execute a variety of functions: act as a protective barrier against adverse environmental conditions (such as situations of extreme temperatures or harmful UV radiation), serve as weapons in hunting prey or for protection against predators, and act as key factors in many other life-sustaining processes and biogeochemical cycles. The unique and complex structures of many marine metabolites enable the discovery of new applications with economic interest (Rotter, et al., 2021).

New bioactives derived from marine biomolecules are especially important for pharmaceutical purposes and can have a plethora of applications. They can be used as antibacterial/antiviral, anti-inflammatory, neuroprotective and anticancer agents. The first marine-derived drugs approved by the Food and Drug Administration (also known as FDA, a government agency established in 1906 that oversees the manufacturing and distribution of food, pharmaceuticals, medical devices, and other products in the United States of America) were the drugs cytarabine (Ara-C) and vidarabine (Ara-A), which are synthetic pyrimidine and purine nucleosides, respectively. Cytarabine was approved in 1969 as an anticancer drug and vidarabine was approved in 1976 as an antiviral agent. Both these drugs were developed from naturally occurring nucleosides isolated from the Caribbean sponge (*Tethya crypta*). The first marine derived anticancer agent to gain approval by the European Union (in 2007) was trabectedin which is used for the treatment of sarcomas and ovarian cancer. Trabectedin is a marine alkaloid extracted from the species *Ecteinascidia turbinata* also known as mangrove tunicate (Montaser & Luesch, 2011).

The examples provided above show that the possibility for new marine pharmaceuticals keeps growing as the current wave of marine life studies allows for the discovery of more novel compounds. Lately the search for these has brought a new perspective in the use of marine venoms. These have been largely ignored as a source for potential drug development, despite research suggesting that there are more marine venomous species than all other venomous terrestrial animals combined. Nonetheless, the variety of biological activities derived from their toxins and other compounds (agglutination, cytotoxicity, coagulation, immunoregulation, etc) make them worth investing in (Xie et al., 2017). With the increase in demand of new products for commercialization, the identification of biomolecules of interest and their function, composition, molecular structure, and acting pathway are therefore pivotal. Notably, biological toxins, which can be defined as antigenic proteins produced by living organisms (Wilson, L. (2023) stand out in this regard. Their chemical and biological diversity is vast, rendering them an exceptional reservoir for uncovering new medications.

1.2 Venomous animals: physiology, ecology and evolution

Before diving in the complexity of venomous animals, the different venom apparatuses they use and the way the main toxins act on upon envenomation of their prey, a quick explanation is needed to better understand the difference between the terms poison and venom since a review of the literature reveals

inconsistency in their definitions. Firstly, both venoms and poisons are comprised of one or more toxins that can vary from small molecular compounds to complex proteins and are able to interfere and disrupt the physiological processes of other organisms and favour their own struggles for existence (Dongwuxue Yanjiu. 2015). Venom toxins are produced in specialized tissues and delivered to the target animal through various venom apparatuses, such as stingers and fangs, in order to exert their effect (Gwaltney-Brant, S. M., 2011). Poison toxins, on the contrary, are produced as secondary metabolic products that accumulate in the host's tissues. The poisonous organisms exert their effect when some of their tissues come into contact with a different organism via ingestion or direct contact (Gwaltney-Brant, S. M., 2011). Therefore, from the standpoint of the toxic organisms, poisoning is mostly a passive process whereas envenomation is an active process where the venomous organisms intentionally deliver their toxins in the respective target (Gwaltney-brant, 2017).

Depending on the animal and its surroundings, venoms can have a variety of functions, which are not necessarily mutually exclusive. Predation is arguably the most common one especially regarding the more known venomous animals namely spiders, scorpions, and snakes. These animals usually use their venom to immobilize or incapacitate prey in order to consume them, in some cases even killing them, that being usually not the case since killing requires higher quantities of venom which is energetically expensive to produce (Schendel, V., et al., 2019). The incapacitation of prey can be caused by two different mechanisms: i) alteration of blood vessels causing blood loss and associated shock, or ii) interference with nerve action causing paralysis. Some studies even consider some venoms to act as aid in digestion using a variety of proteolytic enzymes (Arbuckle, 2017). Defence is another function. Most venomous animals can use venom in a defensive manner while still being predators, however some others use it primarily as a defence mechanism, for example bees. Intraspecific competition, although rarely, can also be one of the main functions of venoms. One good example are the nocturnal slow lorises (*Nycticebus*). These mammals possess a venomous bite (produced by the brachial gland and mixed with saliva) that can injure other lorises as an act of territory and mate defence (Nekaris et al., 2020). Some scorpions of the genus *Hadogenes*, besides using their venom for predation or defence, can also use it during courtship where the males will sting females in their sides, which leads to sedative and perhaps aphrodisiac effects (Arbuckle, 2017).

So far more than 100,000 venomous species throughout the animal kingdom were identified, distributed through all major phyla (Calvete, 2009). Venom systems have evolved independently more than 100 times in an extremely wide range of taxa as shown in Figure 1.1 (Schendel, Rash, Jenner, & Undheim, 2019). In each of these lineages, toxins (usually proteins or peptides) have evolved from a non-toxin ancestral (also protein or peptide), which acquired a new function and act on specific biological pathways of cells (Jackson and Koludarov, 2020). In addition, many of these proteins and peptides have been convergently obtained venomous functions in different lineages. The cysteine-rich secretory proteins (CRISP) and Antigen 5 (Ag5), for example, can be found in the venoms of a variety of animals

(snakes, cone snails, scorpions, spiders and many others). Further studying of venoms and their toxins should provide excellent models for the understanding of adaptive evolution processes.

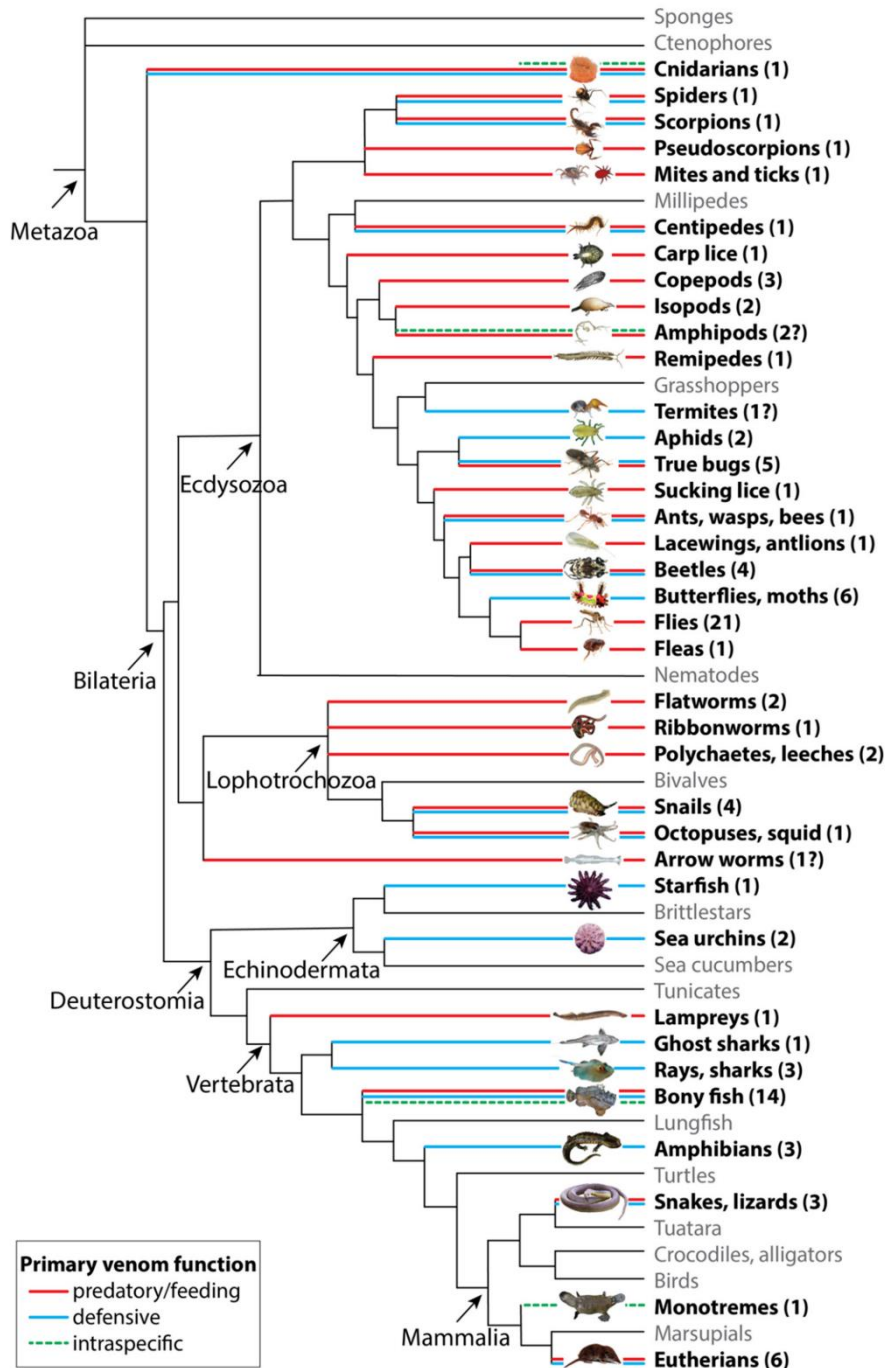


Figure 1.1 Taxonomic diversity and the main primary functions of venom. A schematic phylogenetic tree of venomous animals (source: Schendel, Rash, Jenner, & Undheim, 2019).

Cnidarians (corals, jellyfish, sea anemones, etc) are the oldest extant lineage of venomous animals including around 10,000 species worldwide (Figure 1.2), and despite their simple anatomy, they are

capable of defending themselves from species far more complex than them (Jouiaei, M., et al., 2015). One species from this phylum is the infamous *Chironex fleckeri* also known as Australian box jellyfish, one of the most venomous animals dangerous to humans. Contact with their tentacles in the worst-case scenario can provoke immediate cardiovascular collapse and death within a few minutes after envenomation, due to their potent pore forming toxins, neurotoxins and lipolytic and proteolytic enzymes (Jouiaei et al., 2015). Mollusca too is home to a diverse assemble of venomous animals such as the *Conus* genus snails (which includes over 500 different species). Envenomation in humans is not common, however, when occurring it is likely to happen when naïve divers pick up cones to keep them as souvenirs. These toxins have a variety of neuromuscular effects through glutamate, and serotonin pathways. Some conotoxins exert their effects on sodium, potassium, and calcium ion channels (Kapil, Hendriksen, & Cooper, 2023). Lastly, Chordata has by far the better-known and better studied venomous animals, the snakes. Reptiles such as the king cobras (*Ophiophagus hannah*) and the black mambas (*Dendroaspis polylepis*) are considered to be two of the most venomous snakes in the planet. The black mambas in general have venom which contains a mixture of neurotoxic compounds, including dendrotoxins, fasciculins, and muscarinic toxins.

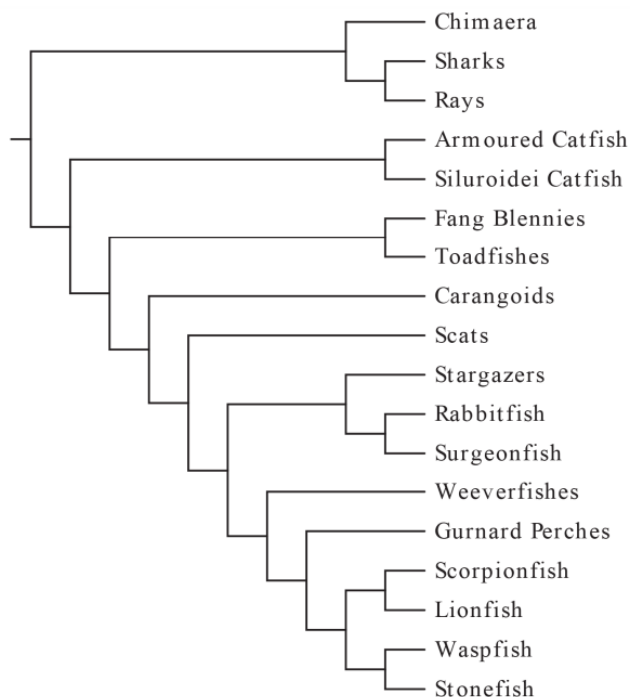


Figure 1.2 A phylogenetic tree showing the known clades of venomous fish (Ziegman & Alewood, 2015).

Also in Chordata, but less represented in the literature we have fish venoms, a largely untapped treasure of biologically important compounds. In Figure 2 the known clades of venomous fishes can be observed. Arguably the *Scorpaenidae* family includes the most venomous fish in the ocean being responsible for many marine envenomations annually (Rensch, G., & Murphy-Lavoie, H. M., 2023). This family can be divided into 3 major subfamilies, *Pteroinae* (lionfish), *Scorpaeninae* (scorpionfish) and *Synanceinae*

(stonefish). All these fish possess spines on their dorsal, pelvic, and anal fins. These spines are encapsulated by glandular venom-producing integumentary sheaths that release venom when mechanically disrupted through contact with their prey/victim (Rensch & Murphy-Lavoie, 2023). The actions of venoms and the specific biological targets of the respective toxins in their compositions is by itself a world on its own. To date not all toxin targets have been identified, and not all the molecular mechanisms underlying the effects of toxins are understood.

1.3 Marine toxins as highly prized bioproducts: applications and opportunities.

Venomomics is the term used to define the characterization of various compounds from animal venoms by using a wide range of omics approaches, including proteomics and genomics. Nowadays, the technologies available allow us to obtain the information about function and structure of hundreds of toxins from snakes, scorpions, spiders, and a plethora of other animals (Da Silva et al., 2014). Toxins, as mentioned earlier, can be defined as toxic substances that are produced by living cells or organisms and are capable of causing disease when introduced into the body (Montecucco & Rossetto, 2014).

So far, toxins have had tremendous impact on drug discovery, due to the incredibly diverse number of biological targets they have. Also, toxins can be used as research tools, for example contributing for a better understanding of the clinical aspects of human envenomation and their respective mechanism of action. Some were successfully used in the creation of new drugs that reached the market. We have drugs for cancer treatment like cytarabine (Cytosar-U®) which was mentioned before, for the treatment of hypertriglyceridemia (fatty acid type drugs; Lovaza®, and Epanova®), for antiviral treatment, (vidarabine (Vira-A®)) and iota-carrageenan (Carragelose®) and many more. Another example of a drug derived specifically from a venomous marine species is ziconotide. A peptide resembling the structure of ω -conopeptide, a toxin discovered in a gastropod of the Conidae family found in the Pacific Ocean (*Conus magus*). This drug was approved by both the FDA in 2004 and the European Union in 2005 and is used in the treatment of severe chronic pain in patients with refractory or intolerant to systemic analgesics or intrathecal morphine (Cappello & Nieri, 2021). Little is known about the composition of marine venoms and, consequently, these venoms present a unique source of novel drugs and scientific research tools. Specially, proteinaceous toxins have an advantage regarding other bioproducts since they can be heterologous expressed by introducing a target gene encoding for a protein of interest from one species into the cell of another species, thus allowing for the host cells to express the foreign protein (Watts, A., Sankaranarayanan, S., Watts, A., & Raipuria, R. K., 2021).

1.4 Weever fishes: marine vertebrates with potential for toxin bi-odiscovery, mechanistic insights and research translation

The weever (or weeverfish) is the name given to the nine extant fish species from the Trachinidae family (from the order Trachiniformes, part of the Percomorpha clade). From those nine species, eight are from the *Trachinus* genus (*T. draco*, *T. araneus*, *T. radiatus*, *T. cornutus*, *T. armatus*, *T. lineulatos*, *T. pellegrini* and *T. collignoni*) and one is from the *Echiichthys* genus (*Echiichthys vipera*). From the nine extant species known, the two main ones are the *Echiichthys vipera* also known as lesser weeverfish and *Trachinus draco*, known as greater weeverfish, both of which occur throughout coastal areas along the Portuguese Exclusive Economic Zone (EEZ).

The lesser weever fish is a small benthonic fish (lives in the bottom of the sea, generally in areas of relatively shallow depths) with silvery skin marked with a yellowish mottled pattern and a black tail (Figure 1.3). The first dorsal fin is also black and made up of five or less venomous spines and a thin membrane in between them. A second dorsal fin runs the length of the rest of the body. Besides the dorsal venomous spines, the species also possesses two other venomous spines, each one located on the right and left operculum that covers the gills (Fig. 1.3). The dorsal spines' grooves that contain the venom glands are lined on the interior of the spine spanning the entirety of their length (Gorman et al., 2020). Lesser weever fishes are mainly distributed through the waters of the northeast Atlantic and Mediterranean Sea and can be found well camouflaged on sandy substrata where they will partially bury themselves revealing their dorsal portions of the body. They are aggressive predators and will snap at small crustaceans such as Mysidacea, Isopoda or Amphipoda or small fish (Teleostei being the main prey) that pass over them (Vasconcelos et al., 2004). In the winter *E. vipera* is mainly found in slightly deeper waters away from the shore. However, during the summer this species migrates into inshore waters (Gorman et al., 2021). This migration during the warmer months makes weeverfish most likely to come into contact with humans. Fishermen can be stung by weever fish in nets when separating the various fishes caught, bathers and other beach users may also step on weevers sometimes when these are buried in sand near to the shore, therefore most envenomations occur to the feet and hands. The most reported symptoms of envenomation include local pain, abdominal pain and inflammation, but nausea and vomiting may also occur (Gorman et al., 2021). So far there was only one recorded death from weever envenomation, where an 18-year-old man was stung on the left leg while snorkelling off the coast of Majorca in Spain. (Borondo et al., 2021).

The method of secretion from the lesser weevers venom glands has been reported as holocrine (secretions are produced in the cytoplasm of cells and released by the rupture of the plasma membrane) and envenomation happens when integumental sheaths surrounding the spines are torn and the venom escapes. (Bonnet, 2000). Its venom contains several thermolabile proteins with high molecular weight,

5-hydroxytryptamine, a protein responsible for the release of histamine, a kinin or kinin-like substance, epinephrine, norepinephrine, histamine, and other enzymes. The toxins found in most piscine venoms are cytolytins also known as pore-forming toxins (around 150 kDa) and possess two subunits, one alpha and one beta and in the case of *E. vipera* that cytolytin is termed trachinine (Gorman et al., 2020).

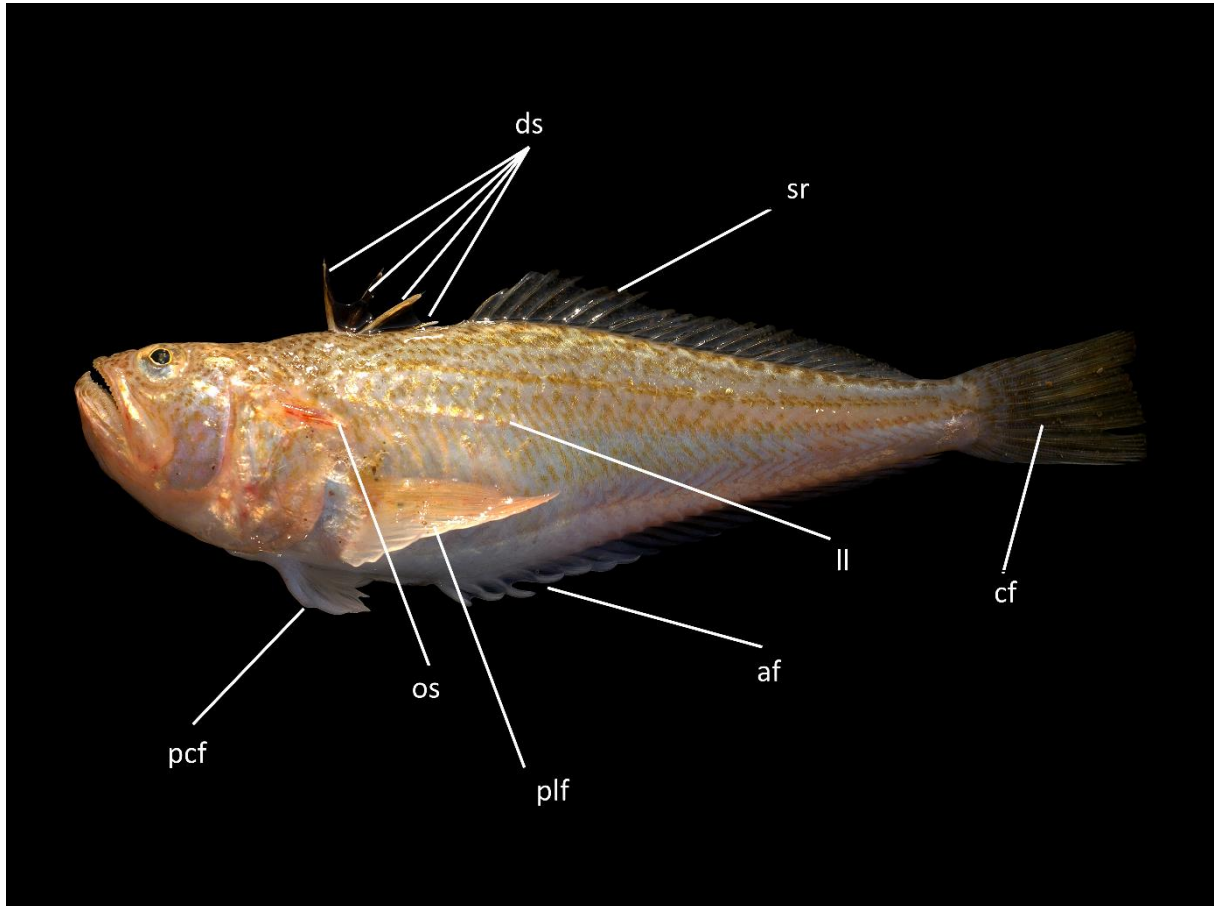


Figure 1.3 Lesser weever (*Echiichthys vipera*). Author Hillewaert, Hans. ds, dorsal spine; sr, soft ray; cf, caudal fin; ll, lateral line; af, anal fin; plf, pectoral fin; os, opercular spine; pcf, pelvic fin.

1.5 Thesis objectives and hypothesis

Although there are already a variety of studies on marine fish venoms and their respective cytolytins, the studies regarding weevers have been rather lacklustre in terms of genomic annotation, which hinders future applications. In addition, little is known about venom and toxin variation in these animals as a function of endogenous variables such as sex, transcriptomic analysis and histology. Therefore, this would be the first study to sequence both the alpha and beta subunits of the *E. vipera*.

The detailed objectives can be summarized as:

- Shortlist the most important proteinaceous toxins in *Echiichthys vipera* venom, identified from qualitative proteomics data previously obtained by SeaTox lab members from venom extracts of *E. vipera* locally collected in Costa da Caparica in 2021.
- Locating, isolating, sequencing and quantifying the expression levels of mRNAs coding for the main toxins, the cytolytic toxin subunits alfa and beta.
- Analysing toxin expression per sex/maturation of fish.
- Describe the venom system of the species with respect to venom secretion and delivery mechanism.

1.6 Thesis relevance to science and society

Acquiring a better understanding for the structure and function of understudied or recently discover toxins as well as obtaining other relevant information such as the genetic sequence of proteinaceous toxins or the way the envenomation apparatus works and how venom is delivered, is an important step towards future drug development.

With the making of this thesis, we help in providing new information for the main important proteinaceous toxins in *Echiichthys vipera* for future use that may help in the production of possible novel drugs.

MATERIALS AND METHODS

2.1 Animals and Sampling

Fish from the species *Echiichthys vipera* were collected by local fisherman from the Costa da Caparica through a traditional artisanal drag-net fishing method called “xávega” during October 2023 and May 2024. The collection was made a long stretch of sandy beaches located in the municipality of Almada along the western coast of the district of Setubal in Portugal (38° 38' 40.49" N, 9° 14' 8.02" W) (Figure 2.1).

The animals were manually sorted from other species and transported to SeaTox laboratory facilities at NOVA-FCT (5 min drive) in aerated tanks. Upon arrival, fish were kept in XX L tanks with local beach sand as environmental enrichment (10 fish per tank) and fed ad libitum twice a day with commercial fish feed. Water parameters such as temperature, salinity, ammonia, nitrites, nitrates and pH were monitored either daily (in the two former) or weekly (in the four latter). Tanks were continuously aerated with air-stones and weekly partial water changes of 10% volume were performed. Temperature was maintained at 20 °C using a chiller. Fish were sampled periodically following euthanasia with tricaine anaesthesia and a cervical cut and sized with an average length of 9.30 cm (SD = 0.87) and an average weight of 9.86 g (SD = 3.74). Next, the venomous spines from the operculum and the first dorsal fin, as well as the soft rays from the second dorsal fin (as control/reference since these are not expected to be venomous), were excised for multi-purpose analyses. Spines and rays were all separately collected in 1.5 mL centrifuge tubes and half of the samples were flash frozen in liquid nitrogen and later stored at -80°C for RNA extraction. The remaining samples were reserved for histology.

Lastly, their sex and sexual maturation stage was recorded observing gonads with a stereoscope (Leica Microsystems DM 2500 LED microscope) following the guidelines for the macroscopic identification of maturity stages for mediterranean fish (see Ungaro, 2008).



Figure 2.1 Map of the sampling area (Wikipedia, 2024). *Echiichthys vipera* was collected from the Costa da Caparica (38° 38' 40.49" N, 9° 14' 8.02" W), located in the municipality of Almada along the western coast of the district of Setúbal in Portugal.

2.2 Histology

The spine samples reserved for histology were fixated with four different fixatives (Davidson, paraformaldehyde (PFA), Bouin and Zenker, 3 spines of each type – opercular, dorsal and reference, per fixative). Bouin's solution is made of picric acid, formaldehyde, and acetic acid, and is well suited for preserving soft tissues such as the putative glands we want to observe. Zenker's fixative contains mercuric chloride and acetic acid and preserves fine nuclear detail but requires special handling due to mercury toxicity. PFA, a formaldehyde-based fixative, is often used at 4%, and is widely applied in electron microscopy due to excellent protein preservation and antigen retention. Lastly, Davidson's fixative is composed of a mixture of formalin, ethanol, and acetic acid and offers rapid fixation without significant tissue shrinkage, making it great for delicate samples. Both Davidson and PFA fixation was done overnight followed by 3 x 15 min washes with MQ-water, and a Post-fixation with Osmium tetroxide 0.1 M also overnight. Fixation with Bouin has achieved with a fixation time of 24h and Zenker fixation was during 48h. After fixation all samples followed the same treatment starting with 3 x 15 min washes. Afterwards samples were dehydrated using Acetone, starting with 15 min washes with increasing acetone concentrations (30%, 60%, 70% and 90%), and ending with a 3 x 10 min washes of pure 100% acetone. Next the samples went through the process of intermediate impregnation, where they were placed in different mixtures with a ratio of 2:1, 1:1, and 1:2 of propylene oxide and EPON respectively for 30 minutes each gradually increasing the concentration of EPON. Samples then were submerged in Epon resin and placed in vacuo for 2h. Lastly the samples were placed in casts and immersed in Epon resin and were placed at 60° C in the oven overnight until the resin solidified.

Thereafter, resin blocks were prepared and identified to produce 2 μm sections for each sample using a RM2245 microtome (Leica Biosystems). Each resin section was placed onto a microscope slide and left to dry o/n. After drying, glass slides were heated in at 60°C for 10 minutes, and then stained with toluidine blue by immersion for 30 seconds, then washed with MQ-water 5 times for 5 seconds each. Then the glass plates were reheated at 70°C once again until totally dry. A coverslip was then mounted over the tissue with xylene and DPX resin.

2.3 RNA Extraction

Total RNA was extracted from tissue samples (dorsal spines, opercular spines and soft rays) weighing 20-30 mg with the RNeasy Mini Kit (Qiagen, Hilden, Germany). The tissues collected in 1,5 mL tubes were macerated with liquid nitrogen till a rough powder was formed. Further lysis was achieved adding 10 μL of Proteinase K and 590 μL of RNase free water and incubating for 10 minutes at 55°C. Afterwards, the resulting mixture was suspended on 600 μL of RLT buffer, for lysing cells, (QIAGEN) and disrupted with a pestle, followed by a 12933 G x 3 min centrifugation (using a Gyrozen, model 1248BR bench centrifuge). After removing the supernatant, 500 μL of 100% ethanol was added to each sample. After transferring the entire volume to a RNeasy mini spin column (QIAGEN), a 12933 G x 1 min centrifugation was followed. It was then added 350 μL of buffer RW1, for washing membrane-bound RNA, (QIAGEN), followed by a 12933 G x 1 min centrifugation. 80 μL of incubation mix (10 μL DNase1 and 70 μL buffer RDD, which provides efficient on-column digestion of DNA, were then added and left to sit at room temperature for 15 min. After adding 350 μL of buffer RW1, it was centrifuged at 12933 G x 1 min. 500 μL of buffer RPE, for washing membrane-bound RNA, (QIAGEN) were then added to the column and a centrifugation of 12933 G x 2 min was ensued. After that, 500 μL of buffer RPE was added, followed by a 12933 G x 3 min centrifugation. The column's collection tube was then replaced with a new one, followed by a centrifugation of 15520 G x 3 min. After placing the column in a 1.5 ml tube, elution of RNA was done using 30 μL of RNase free water at 60°C. The tube was then centrifuged at 12933 G x 2 min. The eluted was taken out, added back to the column, and centrifuged once more using the same parameters. The tubes were then kept at -80°C for storage. To determine RNA concentration and purity, 2 μL of each sample were examined on a Nanodrop One spectrophotometer (Thermo Fisher Scientific Inc. Waltham, Massachusetts, EUA) at 260/280 and 260/230 ratios. All RNA extractions were performed in 2023-2024 within the scope of this thesis.

2.4 Reverse transcription of RNA to cDNA

The transcription of RNA samples to cDNA was done using NZY First-Strand cDNA Synthesis Kit following manufacturer's instructions for a total volume of 20 μL per reaction. The following protocol was

used: Priming 10 minutes at 25°C. Reverse transcription 30 minutes at 50°C. RT inactivation 5 minutes at 85°C. RNA removal 20 minutes at 37°C. Finally, cDNA samples were stored at -20°C until further use.

2.5 Primer Design and Testing

Consensus primer pairs for PCR and qRT-PCR were designed from relevant complete and partial Ef1a, GAPDH, cytolysin alfa subunit (Tx-A) and cytolysin beta subunit (Tx-B) mRNA sequences from the GeneBank database, retrieved in FASTA format for further use in MEGA11 program. Sequences were chosen based on relevant species and relevant alignments and previous LC-MS/MS analyses of crude protein extract provided by the SeaTox lab, where the peptide sequences obtained were compared with other amino acid sequences from the GenBank database through BLAST (Altschul, S. F., et al 1990). The BLAST results showed that the small peptide sequences had highest similarity with alfa and beta cytolysin subunits from other known venomous bony fish species like *Sebastiscus marmoratus*. Sequences resembling those from *Echiichthys vipera* were applied for the design of the primers, with the objective of designing primers between 16 and 24 bp (see Table 2.1). Sequences were aligned using the Muscle algorithm available in MEGA 11 (Tamura et al., 2021).

To create and test the primers for the formation of self-dimers, hairpins, and heterodimers as well as predict annealing temperatures, the tools Primer-BLAST (NCBI), OligoAnalyzer™ Tool (Integrated DNA technologies IDT) and PCR Primer Stats (Bioinformatics.org) were used. Primer sequences, product sizes and annealing temperatures are presented in Table 2.2.

Table 2.1 Relevant genes for qPCR tags Accession List. Sequences retrieved from Genebank between October 2023 - May 2024; based on relevant species and relevant alignments.

Accession	Gene ID	Status
MK860172.1	<i>Sander vitreus</i> glyceraldehyde 3-phosphate dehydrogenase (GAPDH)	Partial
MK860171.1	<i>Sander vitreus</i> elongation factor 1 alpha (Ef1a)	Partial
KF156777.1	<i>Echiichthys vipera</i> Tx-Aunit	Complete
AB623221.1	<i>Pterois antennata</i> Tx-B	Complete
KJ689806.1	<i>Scorpaenopsis oxycephala</i> Tx-B	Complete
KJ689808.1	<i>Sebastiscus marmoratus</i> Tx-B	Complete
MG053104.1	<i>Scorpaena plumieri</i> Tx-B	Complete

Table 2.2 Relevant genes for PCR primers used in this paper and their respective sequences, annealing temperature and product sizes.

Gene		Sequence (5'-3')	Annealing temperature (C°)	Product size (bp)
Ef1a (Tag)	Forward	ACTGTTGCCTTTGTCCCAT	53	149
	Reverse	CAAGATAGCATCCAGAGCCTCC		
GAPDH (Tag)	Forward	ACACGCCATCTCTGTCTTCC	53	185
	Reverse	TGACAAACATCGGAGCATCAGG		
Cytolisin Alfa subunit (Tag)	Forward	GAGGGGTTCCGGTCTGTCAA	53	194
	Reverse	ACCAGCCAGACCTTCATTGG		
Cytolisin Beta subunit (Tag)	Forward	AGTTGATGACTCACCTTGAAGC	53	166
	Reverse	ATGCTGCCCTGAATATCCTGAAC		
Cytolisin Beta subunit (partial)	Forward	GTTGGAGTCATGTCTTCAGAAATC	57	815
	Reverse	CCTAAGTATTGGAGTGCTGCTA		

For primer testing we used a mix of 10x PCR MgCl₂ buffer (Invitrogen), dNTPs, MgCl₂ (Invitrogen), DEPC-Treated Water, cDNA extracted previously, TaqDNA polymerase (Invitrogen), and the respective primer pairs (forward and reverse). For PCR amplification a thermocycler was used with the following steps: 40 cycles of denaturation at 94°C for 3 min, annealing at 53 °C for 30 s for primer tags and , annealing at 57 °C for 90 s for the partial sequence primers , and extension at 72 °C for 30 s and an initial 3 min of denaturation at 94 °C, followed by the final 10 min of extension at 72 °C. An agarose gel was prepared by mixing 0,6 g of standard agarose with 50 ml of TAE buffer 1x. The mixture was heated and mixed on a microwave until the agarose melted and the solution homogenized. After cooling, 5 µL of GelRed (EMD Milipore) were added into the solution and it was poured onto a geltray (Clever Scientific Ltd). After solidification, combs were removed and the tray was placed in a gel electrophoresis system (Clever Scientific Ltd), where TAE 1x was poured until the upper limit. Wells were loaded with 1,5 µL of RNA Ladder or 3 µL of sample + 1.5 µL of loading dye. Power output was supplied by a nanoPAC-300P (Clever Scientific) power supply with a voltage of 80V for about 35 min. With the use of UV from Gel Dock, bands from the agarose gel could be identified. The PCR products underwent Sanger sequencing using an ABI 3730 xl sequencer and a BigDye Terminator sequencing kit, both manufactured by Thermo Fischer Scientific.

2.6 Gene Expression Analyses

Quantification of expression of the target genes was performed using a Rotor-Gene Q thermocycler (Qiagen). Assays were performed using 1 μ L cDNA, 0.4 μ L of each primer, 5 μ L of Master Mix and 3,2 μ L of DEPC treated water, for a total volume of 10 μ L.

Blanks consisted of reactions prepared with 5 μ L of Master Mix and 5 μ L of DEPC treated water, for a total volume of 10 μ L. Blanks with primers only were performed with 0.4 μ L of each primer, 5 μ L of Master Mix and 4,2 μ L of DEPC treated water, for a total volume of 10 μ L. The PCR program consisted of 10 min of Taq polymerase activation at 95 °C followed by 50 cycles of 25 s of denaturation at 94 °C, 20 s of annealing at 53 °C and 25 s of extension at 72 °C. Final extension was at 72 °C for 10 min. Melting curves of the respective tag sequences were retrieved for quality assurance (please see appendix A.1). The qRT-PCR products for the Tx A and Tx B sequences underwent Sanger sequencing using an ABI 3730 xl sequencer and a BigDye Terminator sequencing kit, both manufactured by Thermo Fischer Scientific (please see appendix A.2).

2.7 Statistical Analysis

Statistical analyses were computed with R 4.3 (Ihaka & Gentleman, 1996). Data complied with all the assumptions to perform parametric analysis, including normality of data, tested with Shapiro-Wilk's test, and homogeneity of variances, tested with Levene's test, and independence of scores. An ANOVA was used to test the main effects of sex on cytolitic subunit alfa and beta expression, followed by Tukey's Honest Significant Difference test for multiple comparisons. The significance level was set at 0.05 for all analyses (see Appendix A.3).

2.8 Protein Functional analysis

Using the sequences obtained for Tx A (complete sequence already available in the GenBank database) and Tx-B (partial sequence obtained with the design of primers created from the alignment of other sequences from beta subunits from similar species) a protein characterization could be done. The translate tool from the Expasy software suite (SIB Swiss Institute of Bioinformatics) was used for the translation of the nucleotide sequences to protein sequences as well as examine the respective open reading frames, following the use of the InterPro platform from EMBL-EBI for the analysis of the proteins obtained, classifying them into families and predicting domains and important sites.

2.9 Phylogenetic Analysis

Amino acid sequences from the GeneBank database, retrieved in FASTA format for further use in MEGA11, were used together with our Tx B partial protein sequence for a phylogenetic analysis. These

sequences were primarily chosen based on relevant species and relevant alignments (see Table 2.3). These were then aligned using the Muscle algorithm available in MEGA 11 (Tamura et al., 2021). The sequences were analysed by reconstructing a homology-based phylogenetic tree the maximum likelihood method with the following settings: Bootstrap method, 500 bootstrap replications, Jones-Taylor-Thornton model.

Table 2.3 Tx A/Tx B protein sequences Accession List. Sequences retrieved from Genebank between May-September 2024; based on relevant species, relevant alignments and on priority to full-coding.

Accession	Gene ID	Status
AIC84048.1	<i>Scorpaenopsis oxycephala</i> Tx-B	Complete
AIC84047.1	<i>Scorpaenopsis oxycephala</i> Tx-A	Complete
AVI44917.1	<i>Scorpaena plumieri</i> Tx-B	Complete
AVI44916.1	<i>Scorpaena plumieri</i> Tx-A	Complete
AIC84050.1	<i>Sebastiscus marmoratus</i> Tx-B	Complete
AIC84049.1	<i>Sebastiscus marmoratus</i> Tx-A	Complete
BAK18814.1	<i>Pterois volitans</i> Tx-A	Complete
BAK18815.1	<i>Pterois volitans</i> Tx-B	Complete
AHY22717.1	<i>Echiichthys vipera</i> Tx-A	Complete
BBF98486.1	<i>Siganus virgatus</i> Tx-A	Complete
BBF98486.1	<i>Siganus virgatus</i> Tx-B	Complete
BAF41221.1	<i>Synanceia verrucosa</i> Tx-A Neoverrucotoxin	Complete
BAF41222.1	<i>Synanceia verrucosa</i> Tx-B Neoverrucotoxin	Complete
AIC84045.1	<i>Sebastapistes strongia</i> Tx-A	Complete
AIC84046.1	<i>Sebastapistes strongia</i> Tx-B	Complete
XP_022607207.1	<i>Seriola dumerili</i> Tx-A-like	Complete
XP_004565355.2	<i>Maylandia zebra</i> Tx-A-like	Complete
RXN02208.1	<i>Labeo rohita</i> Tx-A-like	Complete
XP_044055412.1	<i>Siniperca chuatsi</i> Tx-B-like	Complete
XP_045925758.1	<i>Micropterus dolomieu</i> Tx-B-like	Complete
XP_043085136.1	<i>Puntigrus tetrazona</i> Tx-B-like	Complete

RESULTS

3.1 Histology

Figures 3.4 and 3.5 depict the morphological characteristics observed in the 3 tissues retrieved from the current study. In the image relevant to the dorsal soft rays (Figure 3.1, A), it is possible to observe 2 dark ossified structures that together make up one soft-ray spine. Around that structure it was possible to identify two different skin layers. The outer skin layer, the epidermis, is composed of epithelial cells, mucous cells (that provide a mucous layer, the primary defence against a variety of pathogenic microbes, that acts as a barrier between the fish and its surroundings since it contains many factors such as lysozymes, and proteases that provide innate immunity) and alarm cells (specialized cells that when ruptured by predators, can reliably indicate the presence of a hunting predator). The inner skin layer, the dermis, is located under the epidermis and the two bony structures that make up the spine, and contains fibroblasts, chromatophores (which are pigment-containing cells), arterioles (small diameter blood vessels that branch out from arteries and lead to capillaries) and venules (small diameter blood vessels that allow blood to return from capillary beds to veins). The two bony structures composing the soft ray in this particular image seem to be detached from the dermis, but this effect is mostly due to the process of fixation itself.

The opercular venomous spine (Figure 3.1, B) exhibited a similar structure compared to the soft ray but this time bony structure appears to be much larger and with a different shape, almost shaped like a mushroom with a large base and two grooves on each side. The epidermis seems to be very similar with the epidermis of the soft rays, the dermis however has a structure not present in the soft rays, a dense mass under the grooves surrounded by the dermis, identified in this study as the putative venomous gland. In this particular case that mass appears to be degraded, and like the soft ray, the opercular spine was detached from the dermis due to the fixation process.

The dorsal venomous spine (Figure 3.1, C) showed a very similar to the opercular spine but with a few differences. The spine, also mushroom shaped with grooves on each side, is slimmer than the opercular one. Also, chromatophores are present in a very large number compared to the other two tissues. The mass

under the spine grooves (venomous glands) appears to be well preserved and divided into various goblet-like structures. In Figure 3.2 we can observe the venomous gland of an opercular spine in more detail.

Venom glands, as seen in Figure 3.2, covered the majority of the inner spine grooves. The cells were arranged closely to one another, and the shape of the cells varied from round to elongated in appearance. The cytoplasm of the cells appeared homogeneous and filled with granules. Among these, some cells were disrupted and discharging granules. Free particles of granules were also observed (Fig. 3.2). In between the large cells, smaller and darker triangle shaped cells were identified.

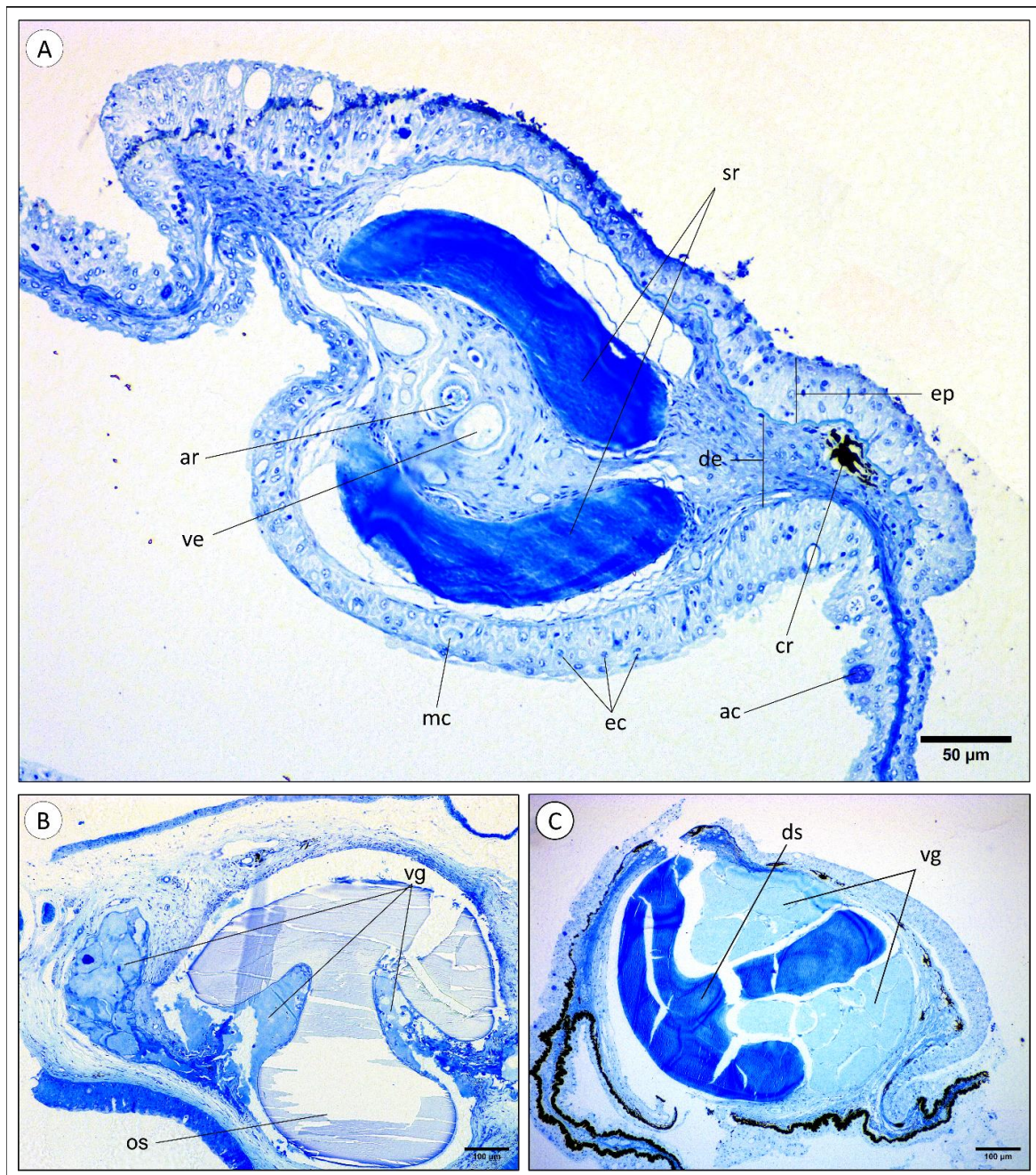


Figure 3.1 Histological images from dorsal and opercular venomous spines and dorsal soft-rays from weever fish *Echiichthys vipera*. **(A)** Dorsal soft ray. Fixation was done with the Bouin's fixative. sr, soft ray; ep, epidermis; de, dermis; cr, chromatophores; ac, alarm cell; ec, epithelial cells; mc, mucous cells; ve, venule; ar, arteriole; **(B)** Opercular venomous spine. Fixation was done with the PFA fixative. os, opercular spine; vg, venomous glands; **(C)** Dorsal venomous spine. Fixation was done with Bouin's fixative. ds, dorsal spine; vg, venomous glands.

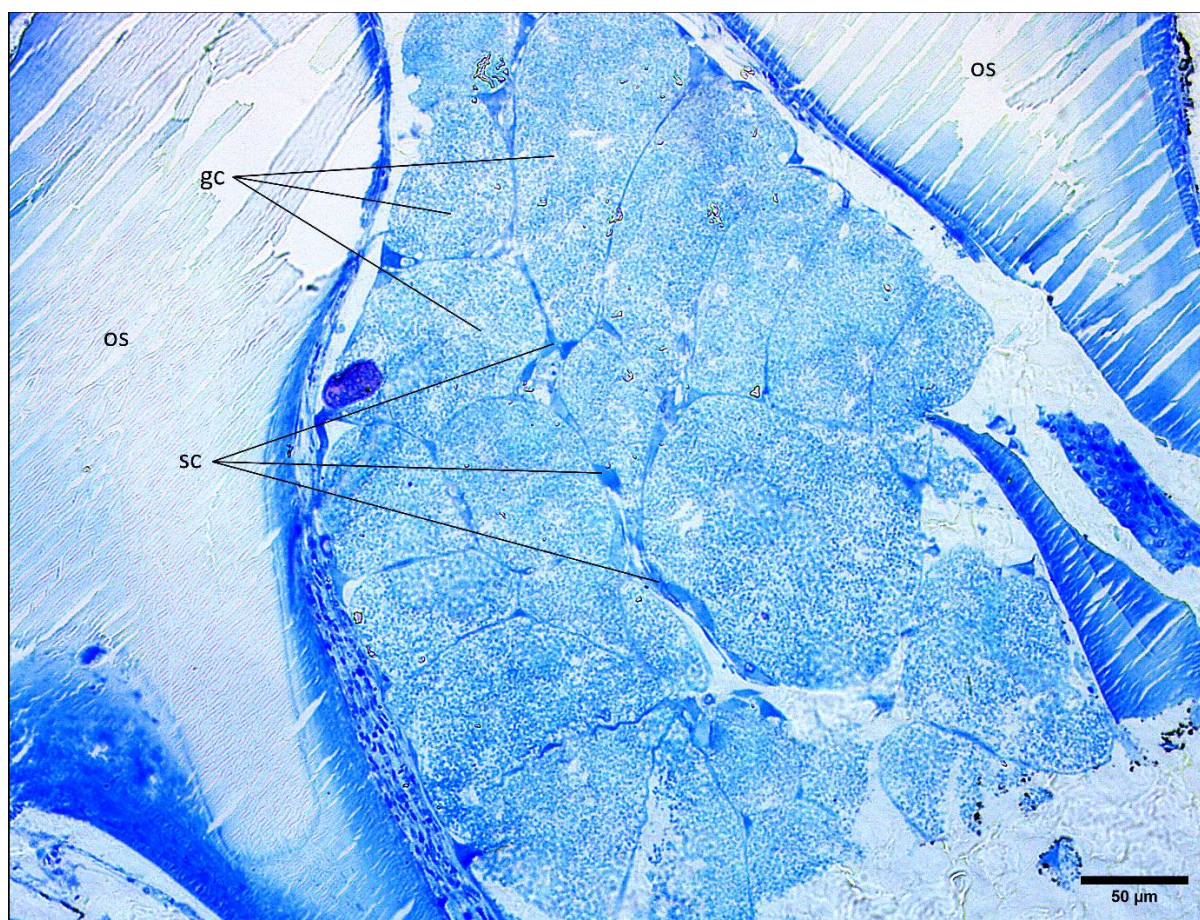


Figure 3.2 Histological image from opercular venomous spine from weever fish *Echiichthys vipera*. Fixation was done with Zenker's fixative and coloration was achieved with toluidine blue. os, opercular spine; gc, gland cell; sc, support cell.

3.2 Toxin subunit alfa and beta Sequence Isolation

After PCR amplification, a band consistent with the expected size for the partial Tx-B product (815 bp), was observed in the first agarose gel for the dorsal spine in lane 4 (Figure 3.3). Lane 1 and 2 contained 15 ng of DNA but were exposed to different annealing temperatures (53 and 51 °C respectively) however showed no bands, while lanes 4 and 5 contained 30 ng of DNA being also exposed to different annealing temperatures (53 and 51 °C respectively) where lane 5 was also exempt of a band. After sequencing, a forward and reverse strand obtained from the lane 4 product was used together with the MEGA11 software to generate a consensus sequence of 815 base pairs (Appendix A.4). This sequence was then subjected to a BLAST analysis (Altschul et al., 1990) comparing it to available sequences. The obtained BLAST results confirmed the correct amplification process, as the retrieved sequences from other specie's cytolyisin beta subunits exhibited the highest similarity to the consensus sequence (as shown in appendix).

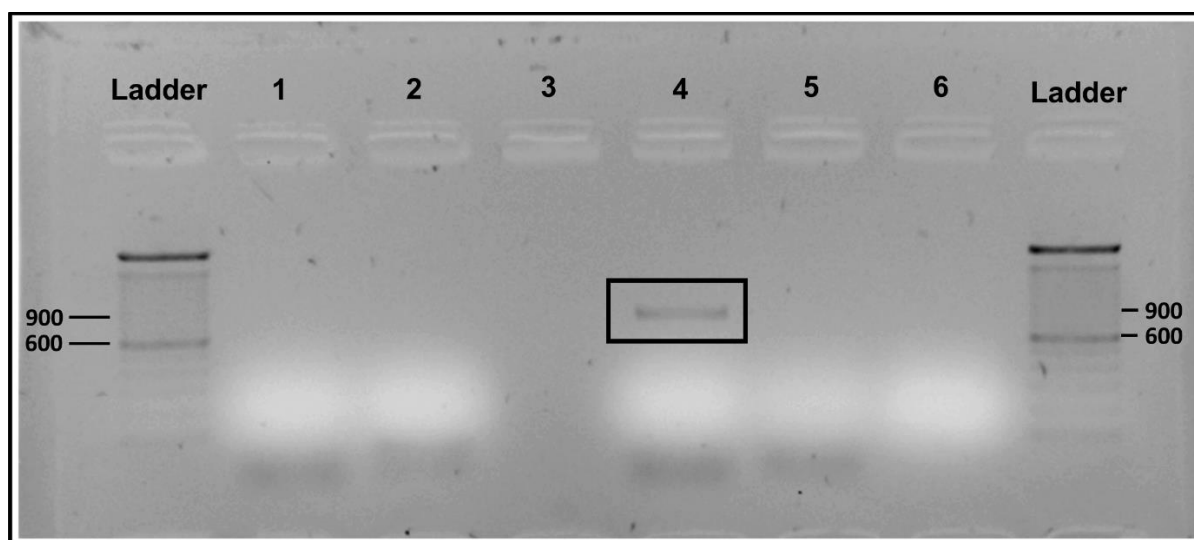


Figure 3.3 Agarose gel electrophoresis of PCR amplified products using cytolysin beta like subunit PCR primers. Lanes 1 and 2 contained 15 ng of cDNA from dorsal spines samples but were exposed to different annealing temperatures (53 and 51 °C respectively). Lanes 4 and 5 contained 30 ng of cDNA from dorsal spines samples but were exposed to different annealing temperatures (53 and 51 °C respectively). Lane 4 presents a band at a mw of 900. Lane 3 consisted of a procedural blank.

With the partial sequence obtained, another PCR amplification was done, where bands consistent with the expect sizes for all the qRT-PCR tag products (149 - 200 bp), were observed in the agarose gel for the dorsal spine in lanes 4, 6 ,10 and 12 (Figure 3.4). Lanes 4 and 6 showed each a band for the two housekeeping genes used (GAPDH and Ef1a) at the desired mw (149 bp-200 bp). The same happened to lanes 10 and 12 for the two genes (Tx-B and Tx-A) showing also the desired mw. Furthermore, negative controls were exempt of bands. After PCR testing, the mentioned primers were used later for qRT-PCR.

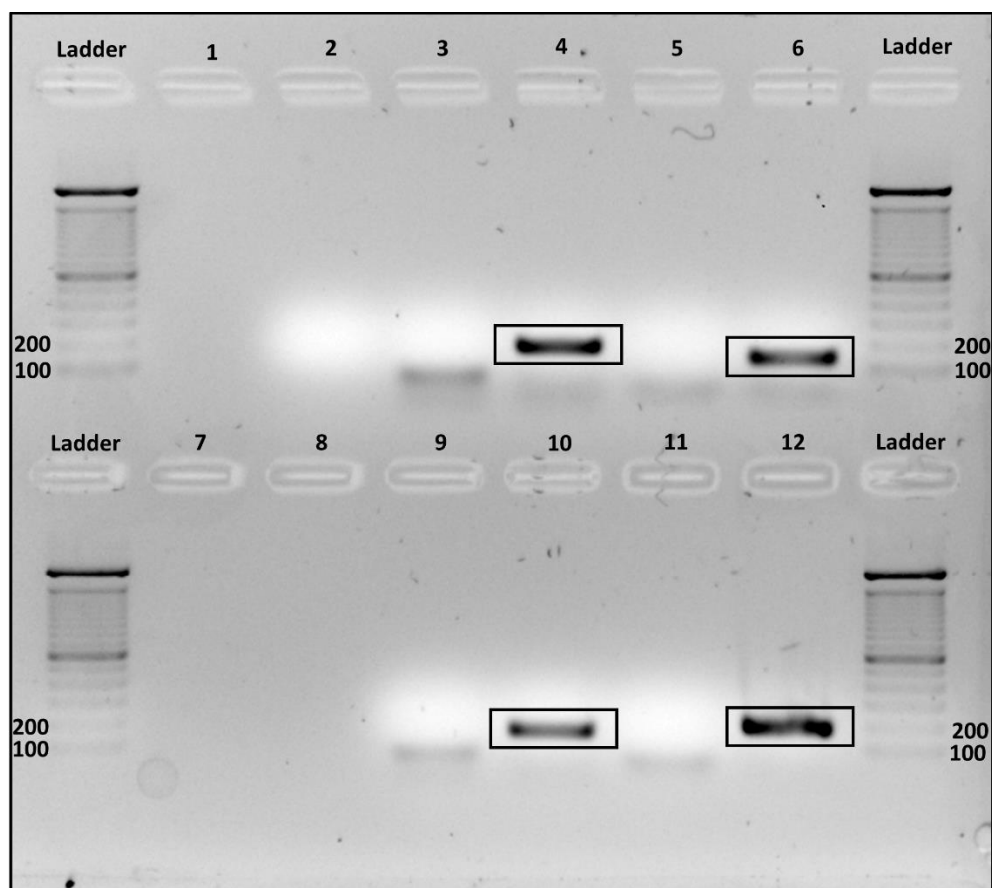


Figure 3.4 Agarose gel electrophoresis of PCR amplified products using qRT-PCR primers. Lanes 1, 7 and 8 are empty. Lane 9 consisted of a procedural blank. Lane 10 and 12 contained the tag products for the housekeeping genes GAPDH and Ef1a, respectively, and lanes 9 and 11 contain the corresponding negative controls for those housekeeping genes. Lanes 10 and 12 contained the tag products for the toxin genes Tx-B and Tx-A, respectively, and lanes 9 and 11 contain the corresponding negative controls.

3.3 Tx A and Tx B Gene Expression

In total, 3 males and 3 females were used for this study. No statistically significant differences were found for the expression of Tx-A and Tx-B relative to Ef1a with ANOVA (Figure 3.5). For the ANOVA of the results from expression of Tx-A and Tx-B relative to GAPDH, the different spines showed statistically significant differences between them (p -value < 0.05) but no differences in expression between sex.

After that a Tukey's test was done to determine which specific group means are different from each other. The test showed statistical significance ($p < 0,05$, Tukey's test) in the expression of Tx B relative to GAPDH between Dorsal spines and Soft rays, and Opercular spines and Soft rays, showing an increase in expression in the venomous spines compared to the Soft rays. The expression of Tx A, when normalised with the housekeeping gene GAPDH showed a statistically significant increase in between the Soft rays and the Opercular spines, but did not exhibit any statistically significant differences ($p > 0,05$, Tukey's test) between the Soft rays and the Dorsal spines.

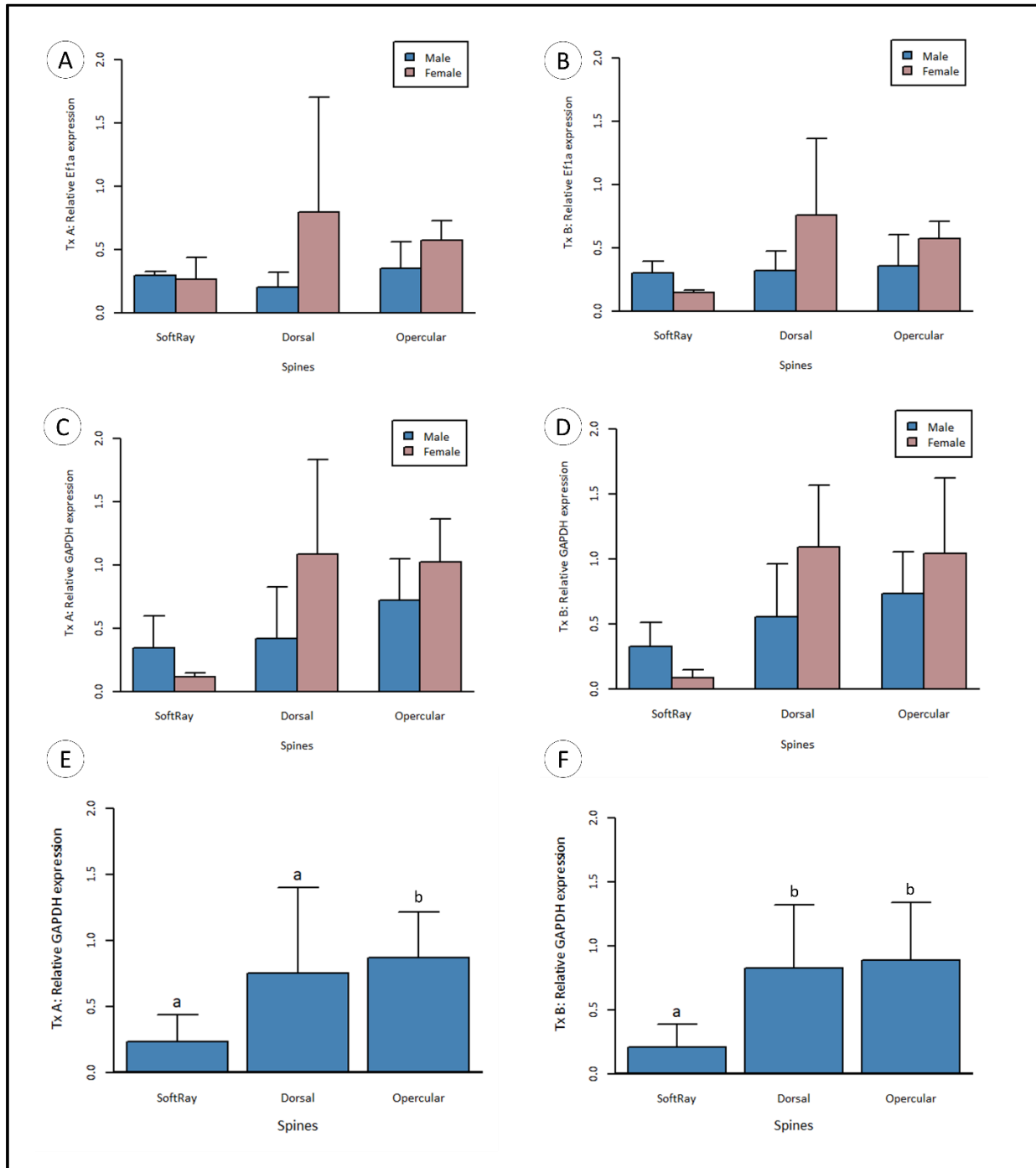


Figure 3.5 Results from all the metrics obtained by qPCR (average from the results of 6 fish, 3 males and 3 females). **(A)** Tx A expression relative to Ef1a; n=3; Male SoftRay (\bar{x} = 0.30; SD = 0.03); Male Dorsal (\bar{x} = 0.21; SD = 0.12); Male Opercular (\bar{x} = 0.35; SD = 0.21); Female SoftRay (\bar{x} = 0.27; SD = 0.17); Female Dorsal (\bar{x} = 0.80; SD = 0.90); Female Opercular (\bar{x} = 0.58; SD = 0.16). **(B)** Tx B expression relative to Ef1a; n=3; Male SoftRay (\bar{x} = 0.31; SD = 0.09); Male Dorsal (\bar{x} = 0.33; SD = 0.15); Male Opercular (\bar{x} = 0.36; SD = 0.25); Female SoftRay (\bar{x} = 0.15; SD = 0.02); Female Dorsal (\bar{x} = 0.76; SD = 0.60); Female Opercular (\bar{x} = 0.58; SD = 0.14). **(C)** Tx A expression relative to GAPDH; n=3; Male SoftRay (\bar{x} = 0.35; SD = 0.25); Male Dorsal (\bar{x} = 0.42; SD = 0.40); Male Opercular (\bar{x} = 0.72; SD = 0.33); Female SoftRay (\bar{x} = 0.11; SD = 0.03); Female Dorsal (\bar{x} = 1.09; SD = 0.75); Female Opercular (\bar{x} = 1.03; SD = 0.34). **(D)** Tx B expression relative to GAPDH; n=3; Male SoftRay (\bar{x} = 0.33; SD = 0.19); Male Dorsal (\bar{x} = 0.56; SD = 0.41); Male Opercular (\bar{x} = 0.73; SD = 0.32); Female SoftRay (\bar{x} = 0.09; SD = 0.06); Female Dorsal (\bar{x} = 1.10; SD = 0.47); Female Opercular (\bar{x} = 1.04; SD = 0.58). **(E)** Tx A expression relative to GAPDH; n=6; SoftRay (\bar{x} = 0.23; SD = 0.20); Dorsal (\bar{x} = 0.76; SD = 0.65); Opercular (\bar{x} = 0.88; SD = 0.34). **(F)** Tx B expression relative to GAPDH; n=6; SoftRay (\bar{x} = 0.21; SD = 0.18); Dorsal (\bar{x} = 0.83; SD = 0.49); Opercular (\bar{x} = 0.89; SD = 0.45). The letters indicate significant differences ($p < 0.05$, Tukey's HSD) between specific pairs of experimental treatments.

3.4 Protein Functional Analysis

Using the available Tx A complete sequence a protein with 704 amino acids was obtained after the use of the Expassy translate tool. Running this protein sequence through InterPro we obtained the following results:

This protein is classified as a cytolytic pore-forming toxin containing 3 representative domains. A stonustoxin_helical domain (being the stonustoxin a large pore forming toxin found in stonefish from the *Synanceia* genus), a Thioredoxin-like SNTX domain (being thioredoxin, also known as THX, a class of small redox proteins present in all organisms that play a role in many biological processes, including redox signalling, and SNTX being the abbreviation given to the pore-forming toxin stonustoxin mentioned before. Lastly, we have the B30.2/SPRY representative domain. This ~200-residue domain is present in a large number of proteins with a variety of individual functions in many different biological processes and is likely to function through protein-protein interactions.

Besides the representative domains we also obtained one of the three Gene Ontology (GO) terms (standardized terms that describe the functions, biological processes, and cellular components associated with proteins or protein domains.) No information was obtained for the biological process and cellular components. For molecular function we obtained protein binding likely due to the presence of the B30.2/SPRY representative domain.

The Tx B partial sequence we obtained was also translated with the Expassy translation tool, obtaining a partial protein sequence with 268 amino acids. Running this partial protein sequence through InterPro we were only able to obtain this protein's family membership, it being also considered a cytolytic pore-forming toxin.

3.5 Phylogeny

The resulting consensus tree was generated based on 500 bootstrap cycles (see Figure 3.6). The examination of eleven Tx A and eleven Tx B homologous proteins from completed and partial amino acid sequences of across various animal taxa, specifically belonging to the most known venomous bony fish Families (*Scorpaenidae*, *Synanceiidae*, *Siganidae*, etc), revealed that the partial Tx B amino acid sequence is closest related to *Siganus virgatus* Tx A (BBF98486.1) and *Siganus virgatus* Tx B (BBF98486.1) and the complete *Echiichthys vipera* Tx-A sequence (AHY22717.1) is most closely related to *Synanceia verrucosa* Tx-A Neoverucocin (BAF41221.1) presenting, however, a low bootstrap value of 41. In this tree, three separate clusters can be observed. One containing Tx A sequences (exception of Tx B from *Pterois volitans*), another with Tx B sequences (exception of Tx A from *Siganus virgatus*), and lastly a cluster containing homologous (alfa and beta) sequences from non-venomous fish.

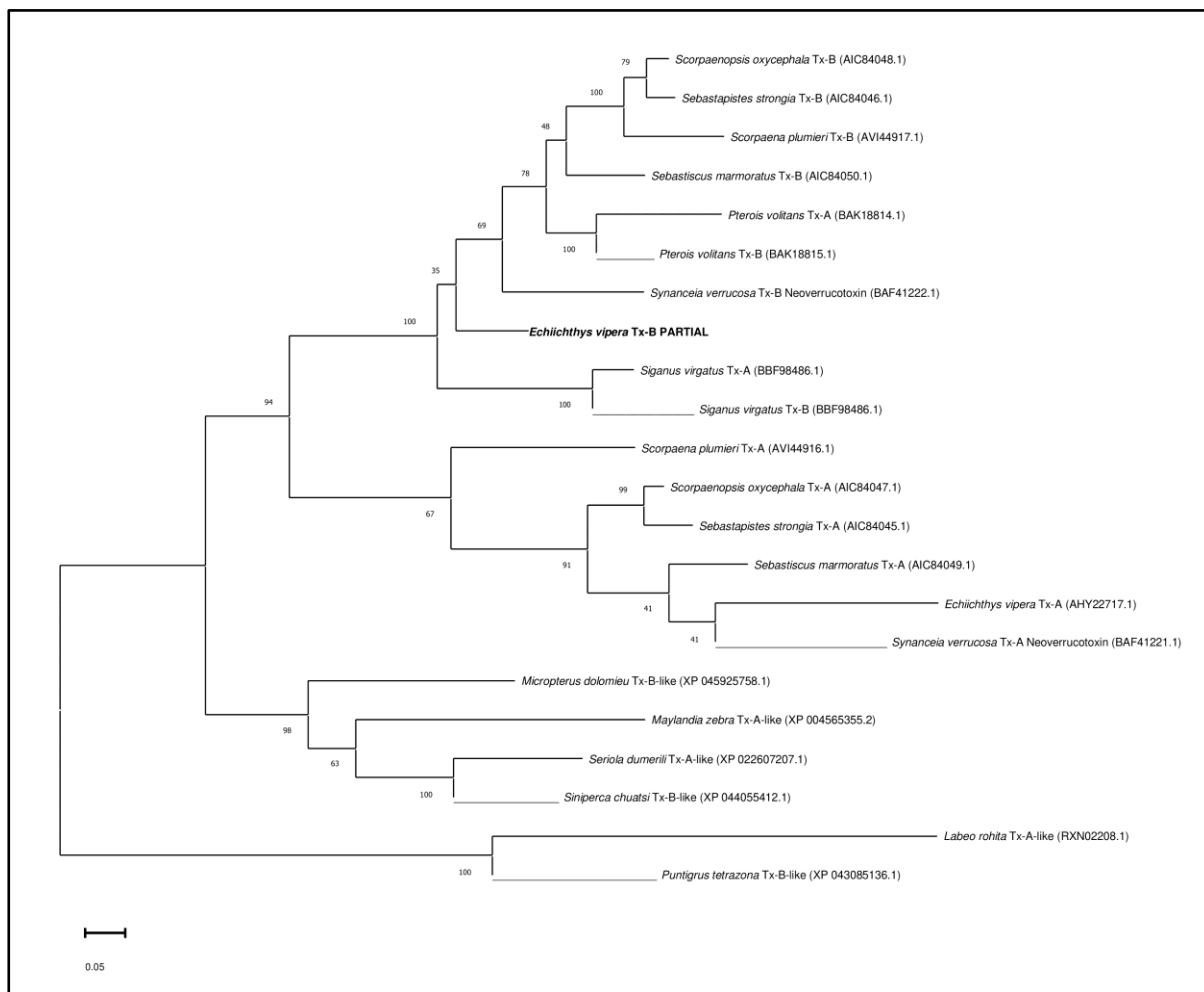


Figure 3.6 Maximum log-likelihood phylogenetic tree allocating 11 cytolitic pore forming toxin alfa subunits and 11 cytolitic pore forming toxin beta subunit amino acid sequences from venomous and non-venomous fish species. The positioning of the partial Tx-B sequence obtained from dorsal spines, of *Echiichthys vipera* in the present study is marked by boldface text. The tree was computed using Maximum Likelihood and the jones-taylor-thornton substitution model, based on 500 bootstrap cycles. The percentage of trees in which the associated taxa clustered together is shown next to the branches. The tree is drawn to scale and the scale bar represents the number of amino acid substitutions per site.

DISCUSSION

The present study suggests the existence of two genes each encoding for one of the two subunits that together form a cytolytic pore-forming toxin in the weever fish *Echiichthys vipera*. One gene is for the alpha subunit (Tx-A) with a length of 2115 bp coding for a protein with 704 amino acids, and the other gene is for the beta subunit (Tx-B) where we were able to sequence the first 815 bp. These two genes were identified in three different tissues: in the soft rays forming the second dorsal fin, in the dorsal spines forming the first dorsal fin, and in the spines located one each in the two operculum.

The histological images obtained were also a major result from this study. In trying to obtain good images the fixative used had a huge impact in what part of the tissues we wanted to preserve. Most important were the dorsal and opercular spines since the fixatives had to penetrate skin and bone in order to reach the glands for preservation. Certain fixatives were great at preserving soft tissues especially the skin which was best preserved with Bouin. In case of the Soft rays (Figure 3.1 A) that were used for comparative purposes, both skin and bony tissue stayed mostly in place maintaining a well-preserved structure. PFA on the other hand had a very hard time reaching the glands resulting sometimes in spines with an unrecognizable mass for glands (Figure 3.1 B). The use of Zenker however resulted in the best results for gland preservation, but did a poor job maintaining the spine structure since it doesn't decalcify bones, meaning that hard bony structures could remain intact but not necessarily well-preserved (Figure 3.2). In terms of morphology, it is possible to admit that both opercular and dorsal spines share a similar structure. Both spines when cut crosswise appear to be T-shaped or rather mushroom shaped surrounded by a small layer of skin (dermis and epidermis) that is retractable and can slide alongside the spine. The skin layer covering the two different spines is fairly similar, but the dorsal one does appear to contain a higher count in chromatophores (or pigment cells), also opercular spines appear to be thicker than dorsal spines but other than that there appear to be no other differences (Figures 3.1 B and C). In between the grooves from the T-shaped spines we can observe the venom glands (Figure 3.2). The glands are lined on the interior of the spine and are divided into large glandular cells each containing many granules inside (possible vesicles containing the proteinaceous toxins and other venom associated molecules). Near the large glandular cells we can observe smaller triangular shaped structures, most likely supporting cells which are likely derived from epidermal cells as mentioned by literature (Gorman et al., 2020). In terms of envenomation process, *Echiichthys vipera* like other venomous fish (like *Synanceia verrucosa*) appears to have a passive venom delivery system meaning it relies on the mechanical force applied to the spines, rather than an active muscle-driven injection (Gorman et al., 2020). The piercing of the venomous spines into a predator probably lead to the displacement of the

skin layer covering the spine groves therefore leaving the glands exposed, leading to the bursting of the glandular cells inside which may result in the leaking of their inner cytoplasmic content, thereby venom secretion be classified as holocrine as other authors indicated before (Gorman et al., 2020). In comparison, scorpionfish contain their glands at the base of the venomous spines and when these spines are pierced into the predator the venom is forced into the wound through a channel running inside the spine (Santhanam, R., 2019 and Saggiomo, S. L., et al., 2021). The features observed for the lesser weever (Fig. 3.5 C) share great similarity with the red lionfish, *Pterois volitans*, where its dorsal fin spines have a try-lobed morphology forming a pair of lateral grooves housing the venomous glands and both the spines and the glandular tissue are covered by a thin membrane, which ruptures when the spines penetrate an object, releasing the venom (Galloway, K. A., & Porter, M. E., 2019).

The lack of studies about reference genes in weever fish is quite a predicament representing an obstacle for the use of qRT-PCR technologies. The lack housekeeping genes sequences for our species (*Echiichthys vipera*) made us rely on the creation of primers for Ef1a and GAPDH genes from *Sander vitreus*, assuming that certain housekeeping genes such as GAPDH, β -actin, 18S rRNA, and tubulin, are often conserved across species due to their essential cellular functions. That said, quantitative gene expression analysis is only reliable when proper reference genes are used for normalization. EF1a and GAPDH were chosen to normalize data since they have been used in the past in other bony fish studies (Dharmaratnam, A., et al 2021). The statistical analysis indicated that from the two housekeeping genes used, only GAPDH normalization showed significant results. A t-test proposed that there was significant difference in the expression of Tx-A in the opercular spine in comparison to the soft rays, however, the ANOVA test showed that there was no difference between the expression of both Tx-A and Tx-B in dorsal/opercular spines and soft rays. On the other hand, expression normalized with GAPDH showed that although there was no statistical significance between both sexes, and between different spine-sex combinations. An increase in the expression of Tx-B was noted when comparing both opercular/dorsal spines to soft rays and an increase of Tx-A expression was noted when comparing opercular spines and soft rays. With all the data obtained some assumptions can be made. Regarding the housekeeping genes chosen, their performance can vary depending on the biological system, tissue type, and experimental conditions. In some cases, Ef1a expression is more susceptible to regulation due to stress or changes in cellular activity, such as during inflammation or in fast-dividing cells (Peña et al., 2010). This can lead to more variability in its qRT-PCR results. GAPDH tends to be more consistently expressed under a variety of conditions, making it more reliable for normalization in many experiments, although it is not universally stable. Also, other differences in qRT-PCR results between housekeeping genes may be due to primer efficiency. If the primers for GAPDH are more efficient or better optimized than those for EF1A, we may observe a better consistency and lower variability in GAPDH expression results. In other words, the stability housekeeping genes can greatly vary depending on the life-stage and/or organ in question.

Regarding toxin expression, we can assume that the fact that toxin expression is not significantly different between males and females suggests that production is likely essential for both sexes and may be tied to basic survival functions, such as defence and predation, or other ecological interactions, rather than sex-specific functions like mating or reproduction. Also, the significant differences across tissues point to the localized production and specialized roles of the toxins in different tissues. This is a common feature for toxic compounds, as many organisms concentrate toxin production in certain organs, in this case the venom glands of the weever fish. Other aspects that may influence that expression may be the maturation stage of the animals used for the study. Since samples were caught in late October and most weevers are mostly underdeveloped during colder seasons, it is possible that venom production is also reduced during this time span. In the future, a more correct approach for a quantitative expression essay would be by separating males and females from the same maturation stage.

Following protein functional analysis, the proteinaceous toxin obtained from the Tx-A showed three representative domains: The Stonustoxin helical domain (from 275 – 368) also found in the two subunits (alfa and beta) that together form the stonustoxin present in stonefish (*Synanceia*). The thioredoxin-like domain or THX domain (from 383 - 506) which is also found in stonustoxin and is comprised of a five-stranded beta-sheet, being thioredoxins small enzymes that are involved in redox reactions via the reversible oxidation of an active centre disulfide bond. Lastly, we have a SPRY/B30.2 domain (from 510 - 704) which is a protein interaction module that can be found in ~100 human proteins and is implicated in important biological pathways (such as regulation of innate and adaptive immunity) and is likely to function through protein-protein interactions (Woo et al., 2006). As described by Campos et al. (2021) the stonustoxin subunits have a THX domain that lacks the canonical catalytic residues which comprise the amino acids located in the active centre of the enzyme responsible for accelerating the enzyme-catalysed reaction by lowering the activation energy of reactions by performing several catalytic functions, therefore, suggesting that the THX domain has a purely structural role. Furthermore, Campos et al. (2021) also established that the SPRY domain was responsible for the initial interaction of the pore forming toxin with the cell surface. In another study (see Ellisdon, A. M., et al., 2015), stonustoxin was analysed using X-ray crystallography, which showed that this toxin is member of an ancient branch of the Membrane Attack Complex-Perforin/Cholesterol-Dependent Cytolysin (MACPF/CDC) superfamily. A detailed protein functional analysis showed that both subunits comprise a THX and a SPRY domain as well as an N-terminal pore-forming MACPF/CDC domain (both are in complex with one another and arranged into a prepore-like assembly) and central focal adhesion-targeting domain also known as FAT. This information provides valuable insight in the action of the cytolytic weever toxin, but further studying is needed for future confirmation.

Following phylogenetic analyses, we focused on our *Echiichthys vipera* Tx-B partial sequence we obtained. Partial sequences may not provide the full evolutionary signal, and their placement in the tree can sometimes be less certain. For example, depending on the length and conservation of the partial sequence, there is a risk that the phylogenetic placement might not fully reflect the evolutionary history

of the complete protein (Lipman, D. J., et al 2002). Also, any functional predictions based solely on this sequence are limited. However, its location in a well-supported clade (bootstrap value 100%) with *Synanceia verrucosa* Tx-B and *Siganus virgatus* Tx-B suggests that despite being a partial sequence, the available portion of the Tx-B subunit in *Echiichthys vipera* shares significant similarity with the Tx-B sequences of these other venomous species, implying a possible conserved function among these proteins. The sequences marked as "Tx-A-like" and "Tx-B-like" (e.g., *Microopterus dolomieu* and *Maylandia zebra*) are homologous sequences from non-venomous fish species. These homologs likely share a common ancestral sequence with the venomous species, but their function has diverged due to the absence of venom in these species. Their placement on the tree, especially on more distant branches forming a clade, shows that while these homologs are evolutionarily related to venom proteins, they have likely undergone functional divergence. Several branches show clear clustering of venomous fish species known for possessing cytolytic toxins. For example, species within the genera *Scorpaenopsis*, *Sebastapistes*, and *Synanceia* cluster together, reflecting their close evolutionary relationships and likely similar toxin profiles. Notably, *Pterois volitans* (the lionfish), a known venomous species, clusters alongside other venomous species, indicating evolutionary relationship. The evolutionary relationships observed here suggest that cytolytic toxins, particularly Tx-A and Tx-B, have evolved in a conserved manner within venomous species, while homologous sequences in non-venomous species have diverged functionally. This pattern reflects the specialization of venom systems in certain lineages, likely driven by selective pressures such as predation or defence, while non-venomous species retained homologous proteins for other biological functions.

CONCLUSIONS AND FUTURE PERSPECTIVES

The current work disclosed the presence of an alfa and a beta subunit gene responsible for the formation of a cytolytic pore forming toxin in the weever fish *Echiichthys vipera* being expressed in the dorsal and opercular venomous spines of the species. Both the dorsal and opercular venom apparatuses possess short bony like spines (3-5 dorsal spines connected by a thin membrane to each other making up the first dorsal spine and one opercular spine in each operculum) that are covered in a thin and retractable layer of skin. A transversal cut through the spines show a T-like shape with two groves, one in each side that harbours the venom glands that appear to be present alongside the entirety of the spine. Envenomation is most likely a passive process caused by the rupture of venom glands when a predator gets empaled by the spines, dislodging the protective layer of skin hiding the glands leading to the bursting of the gland cells and the liberation of the toxins to the predator's blood vessels. This is backed by the lack of muscle tissue near the venom glands. An almost identical envenomation process is found in the venomous lionfish *Pterois volitans*. As for the expression of these subunits, they appear to be focussed on the venomous spines both dorsal and opercular and show no significant differences in between them, also the expression production is likely essential for both sexes and may be tied to basic survival functions, such as defence since it is not significantly different between males and females and is therefore seemingly unrelated to reproduction processes or behaviour. Further studies regarding the expression of alfa and beta subunits in *Echiichthys vipera* should focus on the expression levels from fishes with different maturation stages. To further advance this study with *Echiichthys vipera* future studies should search for: 1) the full coding sequence for the lesser weever cytolytic beta subunit, 2) quantitate the expression levels of toxin mRNAs per maturation stage and other endogenous and environmental variables, 3) the heterologous expression of both Tx A and Tx B, 4) comparative toxicity assessment.

REFERENCES

- Altschul, S. F., Gish, W., Miller, W., Myers, E. W., & Lipman, D. J. (1990). Basic local alignment search tool. *Journal of Molecular Biology*, 215(3), 403–410.
- Arbuckle, K. (2017). Evolutionary Context of Venom in Animals. In *Evolution of Venomous Animals and Their Toxins* (pp. 3–31). Springer Netherlands. https://doi.org/10.1007/978-94-007-6458-3_16
- Bekiari, M. (2023). Marine Bioprospecting: Understanding the Activity and Some Challenges Related to Environmental Protection, Scientific Research, Ethics, and the Law. In: Garcia, M.d.G., Cortês, A. (eds) *Blue Planet Law. Sustainable Development Goals Series*. Springer, Cham. pp 237–252
- Bonnet, M. (2000). The toxicology of *Trachinus vipera*: The lesser weeverfish. In *British Homoeopathic journal* (Vol. 89, Issue 2, pp. 84–88). Georg Thieme Verlag KG. <https://doi.org/10.1054/homp.1999.0359>
- Borondo, J. C., Sanz, P., Nogué, S., Poncela, J. L., Garrido, P., & Valverde, J. L. (2001). Fatal weeverfish sting. In *Human & Experimental Toxicology* (Vol. 20, Issue 2, pp. 118–119). SAGE Publications. <https://doi.org/10.1191/096032701668435659>
- Campos, F. V., Fiorotti, H. B., Coitinho, J. B., & Figueiredo, S. G. (2021). Fish cytolytins in all their complexity. *Toxins*, 13(12), 877. <https://doi.org/10.3390/toxins13120877>
- Cappello, E., & Nieri, P. (2021). From Life in the Sea to the Clinic: The Marine Drugs Approved and under Clinical Trial. In *Life* (Vol. 11, Issue 12, p. 1390). MDPI AG. <https://doi.org/10.3390/life11121390>
- Da Silva, S. L., Rowan, E. G., Albericio, F., Stábeli, R. G., Calderon, L. A., & Soares, A. M. (2014). Animal Toxins and Their Advantages in Biotechnology and Pharmacology. In *BioMed Research International* (Vol. 2014, pp. 1–2). Hindawi Limited. <https://doi.org/10.1155/2014/951561>
- Dharmaratnam, A., Sudhagar, A., Nithianantham, S. R., Das, S., & Swaminathan, T. R. (2021). Evaluation of candidate reference genes for quantitative RTqPCR analysis in goldfish (*Carassius auratus* L.) in healthy and CyHV-2 infected fish. In *Veterinary Immunology and Immunopathology* (Vol. 237, p. 110270). Elsevier BV. <https://doi.org/10.1016/j.vetimm.2021.110270>
- Ellisdon, A. M., Reboul, C. F., Panjekar, S., Huynh, K., Oellig, C. A., Winter, K. L., Dunstone, M. A., Hodgson, W. C., Seymour, J., Dearden, P. K., Tweten, R. K., Whisstock, J. C., & McGowan, S. (2015). Stonefish toxin defines an ancient branch of the perforin-like superfamily. In *Proceedings of the National Academy of Sciences* (Vol. 112, Issue 50, pp. 15360–15365). Proceedings of the National Academy of Sciences. <https://doi.org/10.1073/pnas.1507622112>
- Galloway, K. A., & Porter, M. E. (2019). Mechanical properties of the venomous spines of *Pterois volitans* and morphology among lionfish species. In *Journal of Experimental Biology*. The Company of Biologists. <https://doi.org/10.1242/jeb.197905>

- Gorman, L. M., Judge, S. J., Fezai, M., Jemaà, M., Harris, J. B., & Caldwell, G. S. (2020). The venoms of the lesser (*Echiichthys vipera*) and greater (*Trachinus draco*) weever fish— A review. In *Toxicon*: X (Vol. 6, p. 100025). Elsevier BV. <https://doi.org/10.1016/j.toxcx.2020.100025>
- Gorman, L. M., Judge, S. J., Harris, J. B., & Caldwell, G. S. (2021). Lesser weever fish (*Echiichthys vipera* Cuvier, 1829) venom is cardiotoxic but not haemorrhagic. In *Toxicon* (Vol. 194, pp. 63–69). Elsevier BV. <https://doi.org/10.1016/j.toxicon.2021.02.002>
- Gwaltney-Brant, S. M. (2011). Zootoxins. In *Reproductive and Developmental Toxicology* (pp. 765–771). Elsevier. <https://doi.org/10.1016/b978-0-12-382032-7.10056-6>
- Gwaltney-Brant, S. M. (2011). Zootoxins. In *Reproductive and Developmental Toxicology* (pp. 765–771). Elsevier. <https://doi.org/10.1016/b978-0-12-382032-7.10056-6>
- Hojjati-Razgi, A. S., Nazarian, S., Samiei-Abianeh, H., Vazirizadeh, A., kordbacheh, E., & Aghaie, S. M. (2024). Expression of Recombinant Stonustoxin Alpha Subunit and Preparation of poly-clonal antiserum for Stonustoxin Neutralization Studies. In *The Protein Journal* (Vol. 43, Issue 3, pp. 627–638). Springer Science and Business Media LLC. <https://>
- Jackson, T. N. W., & Koludarov, I. (2020). How the Toxin got its Toxicity. In *Frontiers in Pharmacology* (Vol. 11). Frontiers Media SA. <https://doi.org/10.3389/fphar.2020.574925>
- Jouiaei, M., Yanagihara, A., Madio, B., Nevalainen, T., Alewood, P., & Fry, B. (2015). Ancient Venom Systems: A Review on Cnidaria Toxins. In *Toxins* (Vol. 7, Issue 6, pp. 2251–2271). MDPI AG. <https://doi.org/10.3390/toxins7062251>
- Kapil, S., Hendriksen, S., & Cooper, J. S. (2023). Cone Snail Toxicity. In *StatPearls*. StatPearls Publishing.
- Lipman, D. J., Souvorov, A., Koonin, E. V., Panchenko, A. R., & Tatusova, T. A. (2002). The relationship of protein conservation and sequence length. In *BMC Evolutionary Biology* (Vol. 2, Issue 1). Springer Science and Business Media LLC. <https://doi.org/10.1186/1471-2148-2-20>
- Montaser R, Luesch H. Marine natural products: a new wave of drugs? *Future Med Chem*. 2011 Sep;3(12):1475-89.)
- Montaser, R. and Luesch, H. (2011) 'Marine Natural Products: A new wave of drugs?', *Future Medicinal Chemistry*, 3(12), pp. 1475–1489. doi:10.4155/fmc.11.118.
- Montecucco, C., & Rossetto, O. (2014). Biological Toxins. In *Pathobiology of Human Disease* (pp. 175–180). Elsevier. <https://doi.org/10.1016/b978-0-12-386456-7.01414-3>
- N. Ungaro 2008. Field manual on macroscopic identification of maturity stages for the Mediterranean fishery resources. GCP/RER/ITA/MSM-TD-21. MedSudMed TechnicalDocuments No 21: 34 pp.)
- Nekaris, K. A. I., Campera, M., Nijman, V., Birot, H., Rode-Margono, E. J., Fry, B. G., Weldon, A., Wirdateti, W., & Imron, M. A. (2020). Slow lorises use venom as a weapon in intraspecific competition. In *Current Biology* (Vol. 30, Issue 20, pp. R1252–R1253). Elsevier BV. <https://doi.org/10.1016/j.cub.2020.08.084>
- Peña, A. A., Bols, N. C., & Marshall, S. H. (2010). An evaluation of potential reference genes for stability of expression in two salmonid cell lines after infection with either *Piscirickettsia salmonis* or IPNV. *BMC Research Notes*, 3(1). <https://doi.org/10.1186/1756-0500-3-101>
- Rensch G, Murphy-Lavoie HM. Lionfish, Scorpionfish, and Stonefish Toxicity. [Updated 2023 Jul 31]. In: *StatPearls* [Internet]. Treasure Island (FL): StatPearls Publishing; 2024 Jan-. Available from: <https://www.ncbi.nlm.nih.gov/books/NBK482204/>

Rensch, G., & Murphy-Lavoie, H. M. (2023). Lionfish, Scorpionfish, and Stonefish Toxicity. In StatPearls. StatPearls Publishing.

Rotter, A., Barbier, M., Bertoni, F., Bones, A. M., Cancela, M. L., Carlsson, J., Carvalho, M. F., Ceglowska, M., Chirivella-Martorell, J., Conk Dalay, M., Cueto, M., Dailianis, T., Deniz, I., Díaz-Marrero, A. R., Drakulovic, D., Dubnika, A., Edwards, C., Einarsson, H., Erdoğan, A., ... Vasquez, M. I. (2021). The Essentials of Marine Biotechnology. In *Frontiers in Marine Science* (Vol. 8). Frontiers Media SA. <https://doi.org/10.3389/fmars.2021.629629>

Saggiomo, S. L., Firth, C., Wilson, D. T., Seymour, J., Miles, J. J., & Wong, Y. (2021). The Geographic Distribution, Venom Components, Pathology and Treatments of Stonefish (*Synanceia* spp.) Venom. In *Marine Drugs* (Vol. 19, Issue 6, p. 302). MDPI AG. <https://doi.org/10.3390/md19060302>

Santhanam, R. (2019). Venomology of Scorpionfishes. In *Biology and Ecology of Venomous Marine Scorpionfishes* (pp. 263–278). Elsevier. <https://doi.org/10.1016/b978-0-12-815475-5.00004-2>

Schendel, Rash, Jenner, & Undheim, (2019). The Diversity of Venom: The Importance of Behavior and Venom System Morphology in Understanding Its Ecology and Evolution. In *Toxins* (Vol. 11, Issue 11, p. 666). MDPI AG. <https://doi.org/10.3390/toxins11110666>

Schendel, V., Rash, L. D., Jenner, R. A., & Undheim, E. A. B. (2019). The Diversity of Venom: The Importance of Behavior and Venom System Morphology in Understanding Its Ecology and Evolution. In *Toxins* (Vol. 11, Issue 11, p. 666). MDPI AG. <https://doi.org/10.3390/toxins11110666>

Shekh, K., Tang, S., Niyogi, S., & Hecker, M. (2017). Expression stability and selection of optimal reference genes for gene expression normalization in early life stage rainbow trout exposed to cadmium and copper. *Aquatic Toxicology*, 190, 217–227. <https://doi.org/10.1016/j.aquatox.2017.07.009>

Vasconcelos, R., Prista, N., Cabral, H., & Costa, M. J. (2004). Feeding ecology of the lesser weever, *Echiichthys vipera* (Cuvier, 1829), on the western coast of Portugal. In *Journal of Applied Ichthyology* (Vol. 20, Issue 3, pp. 211–216). Hindawi Limited. <https://doi.org/10.1111/j.1439-0426.2004.00547.x>

Wan, M., Qin, W., Lei, C., Li, Q., Meng, M., Fang, M., Song, W., Chen, J., Tay, F., & Niu, L. (2021). Biomaterials from the sea: Future building blocks for biomedical applications. In *Bioactive Materials* (Vol. 6, Issue 12, pp. 4255–4285). Elsevier BV. <https://doi.org/10.1016/j.bioactmat.2021.04.028>

Watts, A., Sankaranarayanan, S., Watts, A., & Raipuria, R. K. (2021). Optimizing protein expression in heterologous system: Strategies and tools. In *Meta Gene* (Vol. 29, p. 100899). Elsevier BV. <https://doi.org/10.1016/j.mgene.2021.100899>

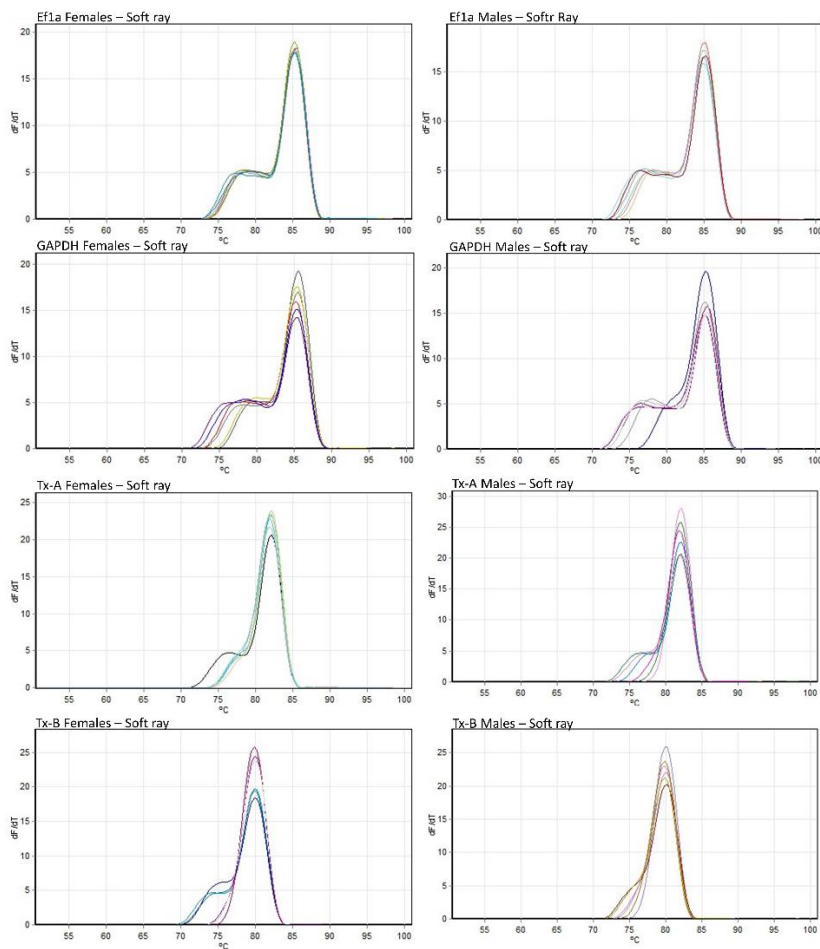
Wilson, L. (2023). Biological Agents: Overview. In *Encyclopedia of Forensic Sciences*, Third Edition (pp. 292–300). Elsevier. <https://doi.org/10.1016/b978-0-12-823677-2.00227-0>

Woo, J., Imm, J., Min, C., Kim, K., Cha, S., & Oh, B. (2006). Structural and functional insights into the B30.2/SPRY domain. *The EMBO Journal*, 25(6), 1353–1363. <https://doi.org/10.1038/sj.emboj.7600994>

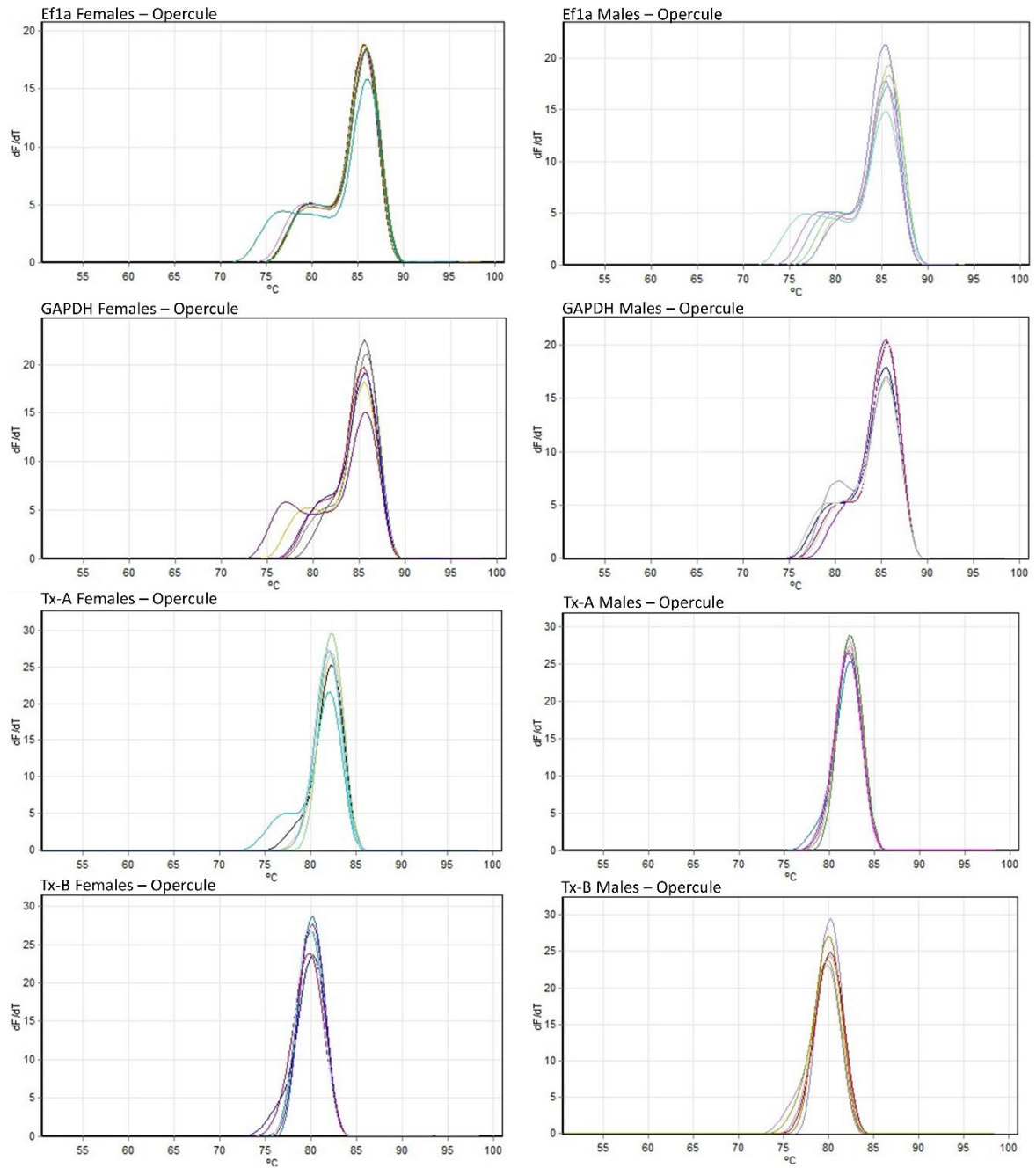
Xie, B., Huang, Y., Baumann, K., Fry, B. G., & Shi, Q. (2017). From Marine Venoms to Drugs: Efficiently Supported by a Combination of Transcriptomics and Proteomics. *Marine drugs*, 15(4), 103. <https://doi.org/10.3390/md15040103>

Ziegman, R., & Alewood, P. (2015). Bioactive Components in Fish Venoms. In *Toxins* (Vol. 7, Issue 5, pp. 1497–1531). MDPI AG. <https://doi.org/10.3390/toxins7051497>

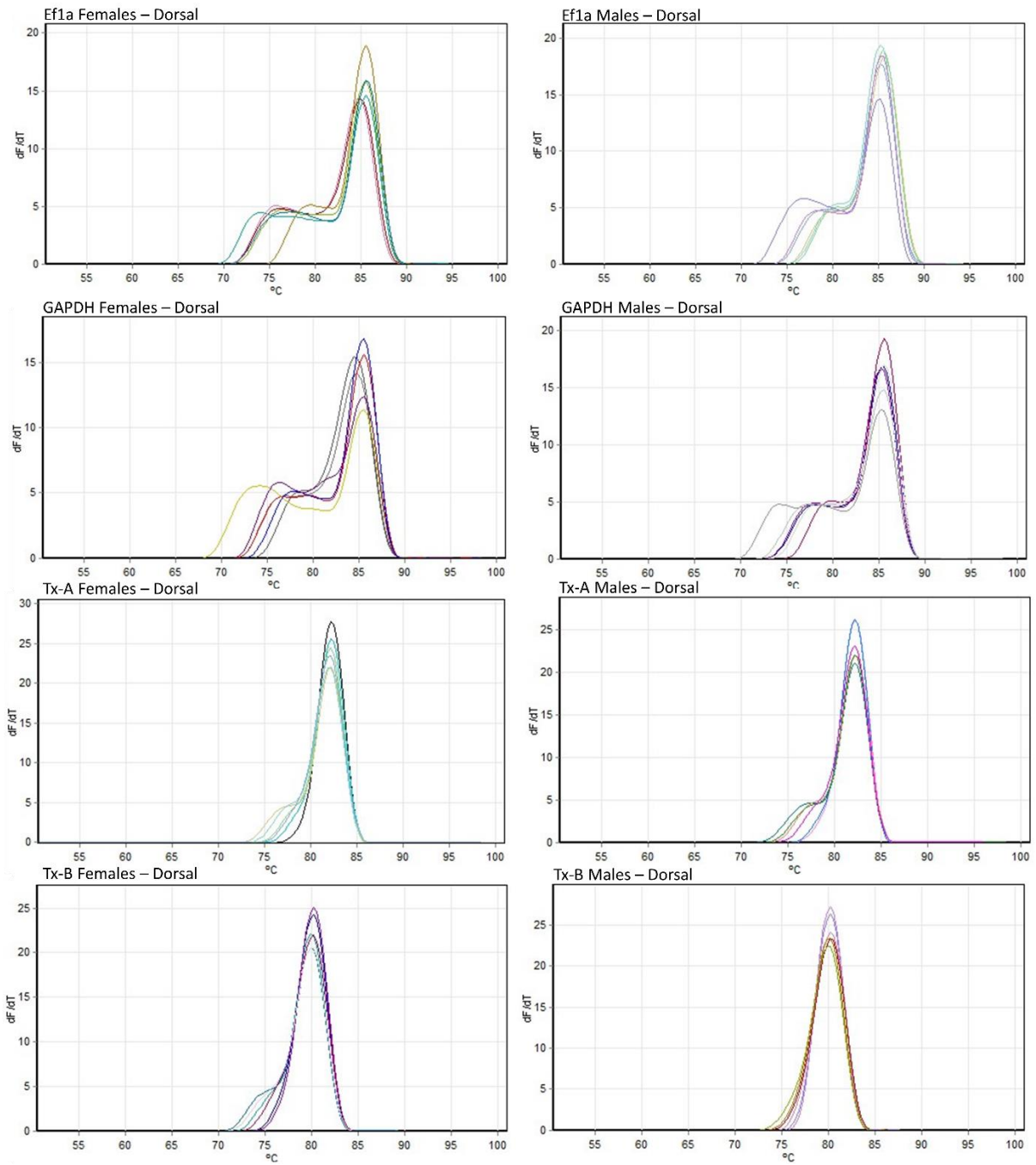
A.1 Melting curves from the qRT-PCR



Appendix A.1.1 Melting curves analysis of qRT-PCR focusing on the Tx-A and Tx-B (plus two housekeeping genes Ef1a and GAPDH) from the second dorsal fin soft rays in *Echiichthys vipera*.



Appendix A.1.2 Melting curves analysis of qRT-PCR focusing on the Tx-A and Tx-B (plus two housekeeping genes Ef1a and GAPDH) from the Opercule spine from *Echiichthys vipera*.



Appendix A.1.3 Melting curves analysis of qRT-PCR focusing on the Tx-A and Tx-B (plus two housekeeping genes Ef1a and GAPDH) from the Dorsal spines from *Echiichthys vipera*.

A.2 Alignments from qRT-PCR products for the Tx-A and Tx-B genes

CLUSTAL W (1.83) multiple sequence alignment. Alfa subunit from soft ray tissue in a Female fish

```
E.vipera_Tx-A  GAGGGGTTTCGGTTCTGTCAAATAACTGATGAAGAAAAAACTCTGGCCAG
SF-C13a        GAGGGGTTTCGGTTCTGTCAAATAACTGATGAAGAAAAAACTCTGGCCAG
*****
```

```
E.vipera_Tx-A  CAATCTCTCCTGCAAGTTTCATGGGGACTTCATCCTTGAAAGCCTCCCTA
SF-C13a        CAATCTCTCCTGCAAGTTTCATGGGGACTTCATCCTTGAAAGCCTCCCTA
*****
```

```
E.vipera_Tx-A  CAACTTTTGAAGATGCAGTGATGACCTACCAGAACTTCCAGAGATTCTT
SF-C13a        CAACTTTTGAAGATGCAGTGATGACCTACCAGAACTTCCAGANATTCTT
***** *****
```

```
E.vipera_Tx-A  GGATCAGATGGATACGAAGGGGTTCCAATGAAGGTCTGGCTGGT
SF-C13a        GGATCAGATGGATACGANGGGGTTCCAATGAAGGTCTGGCTGGT
***** *****
```

CLUSTAL W (1.83) multiple sequence alignment. Alfa subunit from soft ray tissue in a Male fish

```
E.vipera_Tx-A  GAGGGGTTTCGGTTCTGTCAAATAACTGATGAAGAAAAAACTCTGGCCAG
SF-C5a        GAGGGGTTTCGGTTCTGTCAAATAACTGATGAAGAAAAAACTCTGGCCAG
*****
```

```
E.vipera_Tx-A  CAATCTCTCCTGCAAGTTTCATGGGGACTTCATCCTTGAAAGCCTCCCTA
SF-C5a        CAATCTCTCCTGCAAGTTTCATGGGGACTTCATCCTTGAAAGCCTCCCTA
*****
```

```
E.vipera_Tx-A  CAACTTTTGAAGATGCAGTGATGACCTACCAGAACTTCCAGAGATTCTT
SF-C5a        CAACTTTTGAAGATGCAGTGATGACCTACCAGAACTTCCAGANATTCTT
***** *****
```

```
E.vipera_Tx-A  GGATCAGATGGATACGAAGGGGTTCCAATGAAGGTCTGGCTGGT
SF-C5a        GGNTCAGANGGANNGANGGNGTTCCAATGAAGGTCTGGCTGGT
** ***** **  ** * *****
```

CLUSTAL W (1.83) multiple sequence alignment. Alfa subunit from Dorsal spine in a Female fish

```
E.vipera_Tx-A  GAGGGGTTTCGGTTCTGTCAAATAACTGATGAAGAAAAAACTCTGGCCAG
SF-D10a        GAGGGGTTTCGGTTCTGTCAAATAACTGATGAAGAAAAAACTCTGGCCAG
                *****

E.vipera_Tx-A  CAATCTCTCCTGCAAGTTTCATGGGGACTTCATCCTTGAAAGCCTCCCTA
SF-D10a        CAATCTCTCCTGCAAGTTTCATGGGGACTTCATCCTTGAAAGCCTCCCTA
                *****

E.vipera_Tx-A  CAACTTTTGAAGATGCAGTGATGACCTACCAGAACTTCCAGAGATTCTT
SF-D10a        CAACTTTTGAAGATGCAGTGATGACCTACCAGAACTTCCAGANATTCTT
                *****

E.vipera_Tx-A  GGATCAGATGGATACGAAGG-GGTTCCAATGAAGGTCTGGCTGGT
SF-D10a        GGATCAGANGGANCGANGGNGGTTCCAATGAAGGTCTGGCTGGT
                *****  ***  **  *****
```

CLUSTAL W (1.83) multiple sequence alignment. Alfa subunit from Dorsal spine in a Male fish

```
E.vipera_Tx-A  GAGGGGTTTCGGTTCTGTCAAATAACTGATGAAGAAAAAACTCTGGCCAG
SF-D9a         GAGGGGTTTCGGTTCTGTCAAATAACTGATGAAGAAAAAACTCTGGCCAG
                *****

E.vipera_Tx-A  CAATCTCTCCTGCAAGTTTCATGGGGACTTCATCCTTGAAAGCCTCCCTA
SF-D9a         CAATCTCTCCTGCAAGTTTCATGGGGACTTCATCCTTGAAAGCCTCCCTA
                *****

E.vipera_Tx-A  CAACTTTTGAAGATGCAGTGATGACCTACCAGAACTTCCAGAGATTCTT
SF-D9a         CAACTTTTGAAGATGCAGTGATGACCTACCAGAACTTCCAGANATTCTT
                *****

E.vipera_Tx-A  GGATCAGATGGATACGAAGGGGTTCCAATGAAGGTCTGGCTGGT
SF-D9a         GGATCNGANGGATACGANGGGGTTCCAATGAAGGTCTGGCTGGT
                *****  **  *****  *****
```

CLUSTAL W (1.83) multiple sequence alignment. Alfa subunit from Opercular spine in a Female fish

```
E.vipera_Tx-A  GAGGGGTTTCGGTTCTGTCAAATAACTGATGAAGAAAAAACTCTGGCCAG
SF-010a       GAGGGGTTTCGGTTCTGTCAAATAACTGATGAAGAAAAAACTCTGGCCAG
                *****

E.vipera_Tx-A  CAATCTCTCCTGCAAGTTTCATGGGGACTTCATCCTTGAAAGCCTCCCTA
SF-010a       CAATCTCTCCTGCAAGTTTCATGGGGACTTCATCCTTGAAAGCCTCCCTA
                *****

E.vipera_Tx-A  CAACTTTTGAAGATGCAGTGATGACCTACCAGAACTTCCAGAGATTCTT
SF-010a       CAACTTTTGAAGATGCAGTGATGACCTACCAGAACTTCCAGAGATTCTT
                *****

E.vipera_Tx-A  GGATCAGATGGATACGAAGGGGTTCCAATGAAGGTCTGGCTGGT
SF-010a       GGATCAGATGGATACGAAGGGGTTCCAATGAAGGTCTGGCTGGT
                *****
```

CLUSTAL W (1.83) multiple sequence alignment. Alfa subunit from Opercular spine in a Male fish

```
E.vipera_Tx-A  GAGGGGTTTCGGTTCTGTCAAATAACTGATGAAGAAAAAACTCTGGCCAG
SF-011a       GAGGGGTTTCGGTTCTGTCAAATAACTGATGAAGAAAAAACTCTGGCCAG
                *****

E.vipera_Tx-A  CAATCTCTCCTGCAAGTTTCATGGGGACTTCATCCTTGAAAGCCTCCCTA
SF-011a       CAATCTCTCCTGCAAGTTTCATGGGGACTTCATCCTTGAAAGCCTCCCTA
                *****

E.vipera_Tx-A  CAACTTTTGAAGATGCAGTGATGACCTACCAGAACTTCCAGAGATTCTT
SF-011a       CAACTTTTGAAGATGCAGTGATGACCTACCAGAACTTCCAGAANTTCTT
                *****

E.vipera_Tx-A  GGATCAGATGGATACGAAGGGGTTCCAATGAAGGTCTGGCTGGT
SF-011a       GGATCAGANGGANNGANGGNGTTCCAATGAAGGTCTGGCTGGT
                ***** **  **  ** *****
```

CLUSTAL W (1.83) multiple sequence alignment. Beta subunit from soft ray tissue in a Female fish

```
E.vipera_Tx-B  AGTTGATGACTCACCTTGAAGCAAGCATGTAGAATATTCTGAATTATTC
SF-C15b        AGTTGATGACTCACCTTGAAGCAAGCATGTAGAATATTCTGANTNATTC
                ***** * ****

E.vipera_Tx-B  GAGAGCATCAAAGCAACTCATGTAGTGATAGGGATCCTTTATGGGGCCAA
SF-C15b        GAGAACATCACAGNAACTCATGTAGTGATAGGGATCCTTTATGGGGCCAA
                ****  ****  ** *****

E.vipera_Tx-B  TGCTTTCTTCGTCTTTGACAGTGACAAAGTAGATTCTAGCAACG TTCAGG
SF-C15b        TGCTTTCTTTGTCTTTGACAGTGACAAAGTAGATTCTAGCAACG TTCAGG
                ***** *****

E.vipera_Tx-B  ATATTCAGGGCAGCAT
SF-C15b        ATATTCAGGGCAGCA-
                *****
```

CLUSTAL W (1.83) multiple sequence alignment. Beta subunit from soft ray tissue in a Male fish

```
E.vipera_Tx-B  AGTTGATGACTCACCTTGAAGCAAGCATGTAGAATATTCTGAATTATTC
SF-C5b        AGTTGATGACTCACCTTGAAGCAAGCATGTNGAATATTCTGAGTNATTC
                ***** ***** * ****

E.vipera_Tx-B  GAGAGCATCAAAGCAACTCATGTAGTGATAGGGATCCTTTATGGGGCCAA
SF-C5b        GAGAACATCANAGCAACTCATGTAGTGATAGGGATCCTTTATGGGGCCAA
                ****  **** *****

E.vipera_Tx-B  TGCTTTCTTCGTCTTTGACAGTGACAAAGTAGATTCTAGCAACG TTCAGG
SF-C5b        TGCTTTCTTTGTCTTTGACAGTGACAAAGTAGATTCTAGCAACG TTCAGG
                ***** *****

E.vipera_Tx-B  ATATTCAGGGCAGCAT
SF-C5b        ATATTCAGGGCAGCAT
                *****
```

CLUSTAL W (1.83) multiple sequence alignment. Beta subunit from Dorsal spine in a Female fish

```
E.vipera_Tx-B  AGTTGATGACTCACCTTGAAGCAAGCATGTAGAATATTCTGAATTATTC
SF-D10b        AGTTGATGACTCACCTTGAAGCAAGCATGTAGAATATTCTGANTNATTC
                ***** * ****
```

```
E.vipera_Tx-B  GAGAGCATCAAAGCAACTCATGTAGTGATAGGGATCCTTTATGGGGCCAA
SF-D10b        GAGAACATCANAGCAACTCATGTAGTGATAGGGATCCTTTATGGGGCCAA
                **** *  *****
```

```
E.vipera_Tx-B  TGCTTTCTTCGTCTTTGACAGTGACAAAGTAGATTCTAGCAACGTTTCAGG
SF-D10b        TGCTTTCTTTGTCTTTGACAGTGACAAAGTAGATTCTAGCAACGTTTCAGG
                ***** *  *****
```

```
E.vipera_Tx-B  ATATTCAGGGCAGCAT
SF-D10b        ATATTCAGGGCAGCAT
                *****
```

CLUSTAL W (1.83) multiple sequence alignment. Beta subunit from Dorsal spine in a Male fish

```
E.vipera_Tx-B  AGTTGATGACTCACCTTGAAGCAAGCATGTAGAATATTCTGAATTATTC
SF-D9b        AGTTGATGACTCACCTTGAAGCAAGCATGTAGAATATTCTGANTCATT
                ***** *  ***
```

```
E.vipera_Tx-B  GAGAGCATCAAAGCAACTCATGTAGTGATAGGGATCCTTTATGGGGCCAA
SF-D9b        GANANCNTCACAGNAACTCATGTAGTGATAGGGATCCTTTATGGGGCCAA
                ** * * *** *  *****
```

```
E.vipera_Tx-B  TGCTTTCTTCGTCTTTGACAGTGACAAAGTAGATTCTAGCAACGTTTCAGG
SF-D9b        TGCTTTCTTTGTCTTTGACAGTGACAAAGTAGATTCTAGCAACGTTTCAGG
                ***** *  *****
```

```
E.vipera_Tx-B  ATATTCAGGGCAGCAT
SF-D9b        ATATTCAGGGCAGCAT
                *****
```

CLUSTAL W (1.83) multiple sequence alignment. Beta subunit from Opercular spine in a Female fish

```
E.vipera_Tx-B  AGTTGATGACTCACCTTGAAGCAAGCATGTAGAATATTCTGAATTATTC
SF-010b        AGTTGATGACTCACCTTGAAGCAAGCATGTAGAATATTCTGAATNATTC
                *****
```

```
E.vipera_Tx-B  GAGAGCATCAAAGCAACTCATGTAGTGATAGGGATCCTTTATGGGGCCAA
SF-010b        GAGAACATCANAGCAACTCATGTAGTGATAGGGATCCTTTATGGGGCCAA
                **** *****
```

```
E.vipera_Tx-B  TGCTTTCTTCGTCTTTGACAGTGACAAAGTAGATTCTAGCAACGTTTCAGG
SF-010b        TGCTTTCTTTGTCTTTGACAGTGACAAAGTAGATTCTAGCAACGTTTCAGG
                *****
```

```
E.vipera_Tx-B  ATATTCAGGGCAGCAT
SF-010b        ATATTCAGGGCAGCAT
                *****
```

CLUSTAL W (1.83) multiple sequence alignment. Beta subunit from Opercular spine in a Male fish

```
E.vipera_Tx-B  AGTTGATGACTCACCTTGAAGCAAGCATGTAGAATATTCTGAATTATTC
SF-011b        AGTTGATGACTCACCTTGAAGCAAGCATGTNGAATATTCTGANTCATT
                *****
```

```
E.vipera_Tx-B  GAGAGCATCAAAGCAACTCATGTAGTGATAGGGATCCTTTATGGGGCCAA
SF-011b        GANAACNTCACAGNAACTCATGTAGTGATAGGGATCCTTTATGGGGCCAA
                ** * * ** * *****
```

```
E.vipera_Tx-B  TGCTTTCTTCGTCTTTGACAGTGACAAAGTAGATTCTAGCAACGTTTCAGG
SF-011b        TGCTTTCTTTGTCTTTGACAGTGACAAAGTAGATTCTAGCAACGTTTCAGG
                *****
```

```
E.vipera_Tx-B  ATATTCAGGGCAGCAT
SF-011b        ATATTCAGGGCAGCAT
                *****
```

A.3 R Scripts

GAPDH Script

```
library(gplots)
library(car)
library(RColorBrewer)
Spider <- read.csv2("C:/Users/pires/Desktop/R Scripts/GAPDH RE com log.csv", sep=";")

class(Spider)
head(Spider)
View(Spider)

#####
#Now convert my values to factors or numeric
Spider$Spine <- as.factor(Spider$Spine)

Spider$Lenght <- as.numeric(Spider$Lenght)
Spider$Weight <- as.numeric(Spider$Weight)
Spider$Sex <- as.factor(Spider$Sex)
Spider$Maturation <- as.factor(Spider$Maturation)

Spider$RE.A <- as.numeric(Spider$RE.A)
Spider$RE.B <- as.numeric(Spider$RE.B)

#####
#Testing aggregate function

RE.A.means <- aggregate(data=Spider, RE.A~Spine, mean, na.rm=TRUE)
RE.A.sd <- aggregate(data=Spider, RE.A~Spine, sd, na.rm=TRUE)
RE.A.means
RE.A.sd

RE.B.means <- aggregate(data=Spider, RE.B~Spine, mean, na.rm=TRUE)
RE.B.sd <- aggregate(data=Spider, RE.B~Spine, sd, na.rm=TRUE)
RE.B.means
RE.B.sd

#####

#ORDER OF COLUMNS AND LINES
RE.B.means <- RE.B.means[c(3, 1, 2),]
RE.B.means
RE.B.sd <- RE.B.sd[c(3, 1, 2),]
RE.B.sd

RE.A.means <- RE.A.means[c(3, 1, 2),]
```

```

RE.A.means
RE.A.sd<-RE.A.sd[c(3, 1, 2),]
RE.A.sd

#####
#Round up numbers
#First for RE.B
RE.B.meansSR <- RE.B.means[1,2]
round(RE.B.meansSR, digits=3)

RE.B.meansD <- RE.B.means[2,2]
round(RE.B.meansD, digits=3)

RE.B.meansO <- RE.B.means[3,2]
round(RE.B.meansO, digits=3)

#Now for RE.A
RE.A.meansSR <- RE.A.means[1,2]
round(RE.A.meansSR, digits=3)

RE.A.meansD <- RE.A.means[2,2]
round(RE.A.meansD, digits=3)

RE.A.meansO <- RE.A.means[3,2]
round(RE.A.meansO, digits=3)

#Making subsets of the spines
SpiderSR<-subset(Spider, Spine=="SoftRay")
SpiderSR
SpiderD<-subset(Spider, Spine=="Dorsal")
SpiderD
SpiderO<-subset(Spider, Spine=="Opercular")
SpiderO

SpiderF <- subset(Spider, Sex=="Female")
SpiderF
SpiderM <- subset(Spider, Sex=="Male")
SpiderM

SpiderFSR <- subset(SpiderF, Spine=="SoftRay")
SpiderFSR
SpiderFD <- subset(SpiderF, Spine=="Dorsal")
SpiderFD
SpiderFO <- subset(SpiderF, Spine=="Opercular")
SpiderFO

SpiderMSR <- subset(SpiderM, Spine=="SoftRay")
SpiderMSR
SpiderMD <- subset(SpiderM, Spine=="Dorsal")
SpiderMD
SpiderMO <- subset(SpiderM, Spine=="Opercular")
SpiderMO
#####

```

```

#t-test

ttest1 <- t.test(SpiderSR$RE.A, SpiderD$RE.A)
ttest1

ttest2 <- t.test(SpiderSR$RE.A, SpiderO$RE.A)
ttest2

ttest3 <- t.test(SpiderSR$RE.B, SpiderD$RE.B)
ttest3

ttest4 <- t.test(SpiderSR$RE.B, SpiderO$RE.B)
ttest4

#####
plotLimitsREB<-as.data.frame(
  cbind(
    (RE.B.means[,2]+RE.B.sd[,2]),
    (RE.B.means[,2]-RE.B.sd[,2])
  )
)
colnames(plotLimitsREB)<-c("upper", "lower")
plotLimitsREB
###
plotLimitsREA<-as.data.frame(
  cbind(
    (RE.A.means[,2]+RE.A.sd[,2]),
    (RE.A.means[,2]-RE.A.sd[,2])
  )
)
colnames(plotLimitsREA)<-c("upper", "lower")
plotLimitsREA

#####
#new improvement to the graph REB
windowsFonts(Calibri = windowsFont("Calibri"))
windows(6,5)
par(lwd=2, mar=c(5,5,1,1), family = "Calibri")

RE.Bplot<-barplot2(
  RE.B.means$RE.B,      #y values
  names.arg=RE.B.means$Spine, #x values
  plot.ci=TRUE,        #plot error bars?
  ci.u=plotLimitsREB$upper, #upper limit of error bars
  ci.l=plotLimitsREB$lower, #lower limit of error bars
  col=c("rosybrown", "steelblue", "steelblue"),
  xlab=expression("Spines"),
  ylab=expression("Tx B: Relative GAPDH expression"*"(t-test to sofray)'),
  ylim=c(0, 1.1*round(max(plotLimitsREB$upper,2))),
  lwd=2,
  ci.lwd="2",

```

```

ci.width=0.4,
cex.lab = 1.2,
cex.axis=1
)
#Further graphical elements must be added AFTER 'barplot2'
abline(h=0, lwd=4)

#####
#p-value on graph how to?
#use RE.B.O
statsRE.B.O<-c(
  "",
  # "p = n.s.",
  paste0("p = ", zapsmall(ttest4$p.value, 2))
)

text(
  RE.Bplot[3,1],
  plotLimitsREB$upper+0.1*max(plotLimitsREB$upper),
  statsRE.B.O
)
#####
statsRE.B.D<-c(
  "",
  # "p = n.s.",
  paste0("p = ", zapsmall(ttest3$p.value, 2))
)

text(
  RE.Bplot[2,1],
  plotLimitsREB$upper+0.1*max(plotLimitsREB$upper),
  statsRE.B.D
)

)
##We can save the plot as a high-resolution TIFF file (600 dpi) with "dev.print".
##Otherwise we can just copy or save the plot from the device window as METAFILE or other convenient format..

dev.print(tiff,
  "RE.Bplot.tif",
  width = 12,
  height = 10,
  units = 'cm',
  type="windows",
  res=600
)

#####33
#REA GRAPH
windowsFonts(Calibri = windowsFont("Calibri"))
windows(6,5)
par(lwd=2, mar=c(5,5,1,1), family = "Calibri")

RE.Aplot<-barplot2(
  RE.A.means$RE.A,      #y values

```

```

names.arg=RE.A.means$Spine, #x values
plot.ci=TRUE,      #plot error bars?
ci.u=plotLimitsREA$upper,  #upper limit of error bars
ci.l=plotLimitsREA$lower,  #lower limit of error bars
col=c("rosybrown", "steelblue", "steelblue"),
xlab=expression("Spines"),
ylab=expression("Tx A: Relative GAPDH expression"*(t-test to sofray')),
ylim=c(0, 1.1*round(max(plotLimitsREA$upper,2))),
lwd=2,
ci.lwd="2",
ci.width=0.4,
cex.lab = 1.2,
cex.axis=1
)
#Further graphical elements must be added AFTER 'barplot2'
abline(h=0, lwd=4)

#####
#p-value on graph how to?
#use RE.B.O
statsRE.A.O<-c(
  "",
  # "p = n.s.",
  paste0("p = ", zapsmall(ttest2$p.value, 2))
)

text(
  RE.A.plot[3,1],
  plotLimitsREA$upper+0.1*max(plotLimitsREA$upper),
  statsRE.A.O
)

dev.print(tiff,
  "RE.A.plot.tif",
  width = 12,
  height = 10,
  units = 'cm',
  type="windows",
  res=600
)

#####
statsRE.A.D<-c(
  "",
  # "p = n.s.",
  paste0("p = ", zapsmall(ttest1$p.value, 2))
)

text(
  RE.A.plot[2,1],
  plotLimitsREA$upper+0.1*max(plotLimitsREA$upper),
  statsRE.A.D
)

```

```
#####3
##We can save the plot as a high-resolution TIFF file (600 dpi) with "dev.print".
##Otherwise we can just copy or save the plot from the device window as METAFILE or other convenient format..
```

```
dev.print(tiff,
  "RE.Bplot.tif",
  width = 12,
  height = 10,
  units = 'cm',
  type="windows",
  res=600
)
```

```
#####
#####
#####
```

```
SpiderNew <- cbind(as.factor(paste0(Spider$Spine, Spider$Sex)),Spider)
View(SpiderNew)
colnames(SpiderNew)[1]<-"Condition"
```

```
#####
#####Homogeneity of Variances:#####
leveneTest(data=SpiderNew, RE.A~Condition, center=median)
leveneTest(data=SpiderNew, RE.A~Sex, center=median)
leveneTest(data=SpiderNew, RE.A~Spine, center=median)
```

```
leveneTest(data=SpiderNew, RE.B~Condition, center=median)
leveneTest(data=SpiderNew, RE.B~Sex, center=median)
leveneTest(data=SpiderNew, RE.B~Spine, center=median)
```

```
#####
#####SHAPIRO#Normality:#####
```

```
SRfem <- subset(SpiderNew, Condition=="SoftRayFemale")
SRfem
shapiro.test(SRfem$RE.A)
shapiro.test(SRfem$RE.B)
```

```
SRmas <- subset(SpiderNew, Condition=="SoftRayMale")
SRmas
shapiro.test(SRmas$RE.A)
shapiro.test(SRmas$RE.B)
#####
```

```
Dfem <- subset(SpiderNew, Condition=="DorsalFemale")
Dfem
shapiro.test(Dfem$RE.A)
shapiro.test(Dfem$RE.B)
```

```
Dmas <- subset(SpiderNew, Condition=="DorsalMale")
Dmas
shapiro.test(Dmas$RE.A)
shapiro.test(Dmas$RE.B)
```

```

#####
Ofem <- subset(SpiderNew, Condition=="OpercularFemale")
Ofem
shapiro.test(Ofem$RE.A)
shapiro.test(Ofem$RE.B)

Omas <- subset(SpiderNew, Condition=="OpercularMale")
Omas
shapiro.test(Omas$RE.A)
shapiro.test(Omas$RE.B)

#####
##### ANOVA #####
#####

SpiderAOVA <- aov(data=SpiderNew, RE.A~Spine*Sex)
summary(SpiderAOVA)

SpiderAOVB <- aov(data=SpiderNew, RE.B~Spine*Sex)
summary(SpiderAOVB)

tukeySPIDERa <- TukeyHSD(SpiderAOVA, conf.level = 0.05)
tukeySPIDERa

tukeySPIDERb <- TukeyHSD(SpiderAOVB, conf.level = 0.05)
tukeySPIDERb
#####
#####
SpiderRE.A = Spider[Spider$Sex %in% c("Male"),-c(1,3,4,5,6,8)]
SpiderRE.A

SpiderRE.AFem = Spider[Spider$Sex %in% c("Female"),-c(1,3,4,5,6,8)]
SpiderRE.AFem

SpiderRE.A <- cbind(SpiderRE.A, RE.AFem = SpiderRE.AFem[,2])
SpiderRE.A

meanA <- aggregate(. ~ Spine, SpiderRE.A, mean)
meanA

sdA <- aggregate(. ~ Spine, SpiderRE.A, sd)
sdA

plotmeanA<-rbind( meanA$RE.A, meanA$RE.AFem)

rownames(plotmeanA)<-c("Male", "Female")
colnames(plotmeanA)<-c("Dorsal","Opercular", "SoftRay")
plotmeanA<-plotmeanA[, c(3,1,2)]
plotmeanA

plotsdA <-rbind( sdA$RE.A, sdA$RE.AFem)

rownames(plotsdA)<-c("Male", "Female")

```

```

colnames(plotsdA)<-c("Dorsal","Opercular", "SoftRay")
plotsdA<-plotsdA[, c(3,1,2)]
plotsdA

plotLimitsREA<-as.data.frame(cbind((meanA[,c(2,3)]+sdA[,c(2,3)]),(meanA[,c(2,3)]- sdA[,c(2,3)]))
colnames(plotLimitsREA)<-c("upper","upper","lower","lower")
plotLimitsREA

upperLimitsREA<-c(1.1*round(max(plotLimitsREA$upper,2)))

windowsFonts(Calibri = windowsFont("Calibri"))
windows(6,5)
par(mar=c(5,5,1,1), family = "Calibri", lwd=2)
dataPlot<-barplot2(plotmeanA,
  beside=TRUE,
  legend=TRUE,
  plot.ci=TRUE,
  ci.lwd = 2,
  ci.u=plotmeanA+plotsdA,
  ci.l=plotmeanA,
  col=c("steelblue","rosybrown"),
  lwd=2,
  ylab="Tx A: Relative GAPDH expression",
  ylim=c(0, 1.1*round(max(plotLimitsREA$upper,2))),
  xlab="Spines"
)
abline(h=0, lwd=2)
text( dataPlot,
  plotmeanA+plotsdA+max(4),
  cex=0.8
)

dev.print(tiff,
  "REAPLOT.tif",
  width = 15,
  height = 10,
  units = 'cm',
  type="windows",
  res=600
)

#####
SpiderRE.B = Spider[Spider$Sex %in% c("Male"),-c(1,3,4,5,6,7)]
SpiderRE.B

SpiderRE.BFem = Spider[Spider$Sex %in% c("Female"),-c(1,3,4,5,6,7)]
SpiderRE.BFem

SpiderRE.B <- cbind(SpiderRE.B, RE.BFem = SpiderRE.BFem[,2])
SpiderRE.B

meanB <- aggregate(. ~ Spine, SpiderRE.B, mean)
meanB

```

```

sdB <- aggregate(. ~ Spine, SpiderRE.B, sd)
sdB

plotmeanB<-rbind( meanB$RE.B, meanB$RE.BFem)

rownames(plotmeanB)<-c("Male", "Female")
colnames(plotmeanB)<-c( "Dorsal", "Opercular", "SoftRay")
plotmeanB<-plotmeanB[, c(3,1,2)]
plotmeanB

plotsdB <-rbind( sdB$RE.B, sdB$RE.BFem)

rownames(plotsdB)<-c("Male", "Female")
colnames(plotsdB)<-c( "Dorsal", "Opercular", "SoftRay")
plotsdB<-plotsdB[, c(3,1,2)]
plotsdB

plotLimitsREB<-as.data.frame(cbind((meanB[,c(2,3)]+sdB[,c(2,3)]),(meanB[,c(2,3)]- sdB[,c(2,3)])) )
colnames(plotLimitsREB)<-c("upper", "upper", "lower", "lower")
plotLimitsREB

upperLimitsREB<-c(1.1*round(max(plotLimitsREB$upper,2)))

windowsFonts(Calibri = windowsFont("Calibri"))
windows(6,5)
par(mar=c(5,5,1,1), family = "Calibri", lwd=2)
dataPlot<-barplot2(plotmeanB,
  beside=TRUE,
  legend=TRUE,
  plot.ci=TRUE,
  ci.lwd = 2,
  ci.u=plotmeanB+plotsdB,
  ci.l=plotmeanB,
  col=c("steelblue", "rosybrown"),
  lwd=2,
  ylab="Tx B: Relative GAPDH expression",
  ylim=c(0, 1.1*round(max(plotLimitsREB$upper,2))),
  xlab="Spines"
)
abline(h=0, lwd=2)
text( dataPlot,
  plotmeanB+plotsdB+max(4),
  cex=0.8
)

dev.print(tiff,
  "REBPLOT.tif",
  width = 15,
  height = 10,
  units = 'cm',
  type="windows",

```

```

    res=600
)

#####
#####

plotLimitsREAS<-as.data.frame(
  cbind(
    (RE.A.means[,2]+RE.A.sd[,2]),
    (RE.A.means[,2]-0)
  )
)
colnames(plotLimitsREAS)<-c("upper", "lower")
plotLimitsREAS
#####
letters <- c("a", "a", "α")

windowsFonts(Calibri = windowsFont("Calibri"))
windows(6,5)
par(lwd=2, mar=c(5,5,1,1), family = "Calibri")

RE.A$plot<-barplot2(RE.A.means$RE.A,      #y values
  names.arg=RE.A.means$Spine, #x values
  plot.ci=TRUE,      #plot error bars?
  ci.u=plotLimitsREAS$upper, #upper limit of error bars
  ci.l=plotLimitsREAS$lower, #(NO LIMIT)
  col=c("steelblue", "steelblue", "steelblue"),
  xlab=expression("Spines"),
  ylab=expression("Tx A: Relative GAPDH expression"),
  ylim=c(0, 1.1*round(max(plotLimitsREAS$upper,2))),
  lwd=2,
  ci.lwd="2",
  ci.width=0.4,
  cex.lab = 1.2,
  cex.axis=1)

#Further graphical elements must be added AFTER 'barplot2'
abline(h=0, lwd=4)

#####

text(x = RE.A$plot, y = RE.A.sd$RE.A + RE.A.means$RE.A + 0.1, labels = letters, cex = 1.5)

#text(RE.A$plot[3,1],plotLimitsREAS$upper+0.1*max(plotLimitsREAS$upper))

dev.print(tiff,
  "RE.Aplot.tif",
  width = 12,
  height = 10,
  units = 'cm',
  type="windows",
  res=600

```

```

)
#####

plotLimitsREBS<-as.data.frame(
  cbind(
    (RE.B.means[,2]+RE.B.sd[,2]),
    (RE.B.means[,2]-0)
  )
)
colnames(plotLimitsREBS)<-c("upper", "lower")
plotLimitsREBS
#####
letters <- c("a", "α", "α")

windowsFonts(Calibri = windowsFont("Calibri"))
windows(6,5)
par(lwd=2, mar=c(5,5,1,1), family = "Calibri")

RE.B$plot<-barplot2(RE.B.means$RE.B,      #y values
  names.arg=RE.B.means$Spine, #x values
  plot.ci=TRUE,      #plot error bars?
  ci.u=plotLimitsREBS$upper,  #upper limit of error bars
  ci.l=plotLimitsREBS$lower,  #(NO LIMIT)
  col=c("steelblue", "steelblue", "steelblue"),
  xlab=expression("Spines"),
  ylab=expression("Tx B: Relative GAPDH expression"),
  ylim=c(0, 1.1*round(max(plotLimitsREBS$upper,2))),
  lwd=2,
  ci.lwd="2",
  ci.width=0.4,
  cex.lab = 1.2,
  cex.axis=1)

#Further graphical elements must be added AFTER 'barplot2'
abline(h=0, lwd=4)

#####

text(x = RE.B$plot, y = RE.B.sd$RE.B + RE.B.means$RE.B + 0.1, labels = letters, cex = 1.5)

#text(RE.A$plot[3,1],plotLimitsREAS$upper+0.1*max(plotLimitsREAS$upper))

dev.print(tiff,
  "RE.Bplot.tif",
  width = 12,
  height = 10,
  units = 'cm',
  type="windows",
  res=600
)

```

```
#####EF1A Script#####
```

```
library(gplots)
```

```
library(car)
```

```
library(RColorBrewer)
```

```
Spider <- read.csv2("C:/Users/pires/Desktop/R Scripts/Final expression with log.csv", sep=";")
```

```
class(Spider)
```

```
head(Spider)
```

```
View(Spider)
```

```
#####
```

```
#Now convert my values to factors or numeric
```

```
Spider$Spine <- as.factor(Spider$Spine)
```

```
Spider$Lenght <- as.numeric(Spider$Lenght)
```

```
Spider$Weight <- as.numeric(Spider$Weight)
```

```
Spider$Sex <- as.factor(Spider$Sex)
```

```
Spider$Maturation <- as.factor(Spider$Maturation)
```

```
Spider$RE.A <- as.numeric(Spider$RE.A)
```

```
Spider$RE.B <- as.numeric(Spider$RE.B)
```

```
#####
```

```
#Testing aggregate function
```

```
RE.A.means <- aggregate(data=Spider, RE.A~Spine, mean, na.rm=TRUE)
```

```
RE.A.sd <- aggregate(data=Spider, RE.A~Spine, sd, na.rm=TRUE)
```

```
RE.A.means
```

```
RE.A.sd
```

```
RE.B.means <- aggregate(data=Spider, RE.B~Spine, mean, na.rm=TRUE)
```

```
RE.B.sd <- aggregate(data=Spider, RE.B~Spine, sd, na.rm=TRUE)
```

```
RE.B.means
```

```
RE.B.sd
```

```

#####
#

#ORDER OF COLUMNS AND LINES
RE.B.means <-RE.B.means[c(3, 1, 2),]
RE.B.means
RE.B.sd <-RE.B.sd[c(3, 1, 2),]
RE.B.sd

RE.A.means <-RE.A.means[c(3, 1, 2),]
RE.A.means
RE.A.sd <-RE.A.sd[c(3, 1, 2),]
RE.A.sd

#####
#

#Round up numbers
#First for RE.B
RE.B.meansSR <- RE.B.means[1,2]
round(RE.B.meansSR, digits=3)

RE.B.meansD <- RE.B.means[2,2]
round(RE.B.meansD, digits=3)

RE.B.meansO <- RE.B.means[3,2]
round(RE.B.meansO, digits=3)

#Now for RE.A
RE.A.meansSR <- RE.A.means[1,2]
round(RE.A.meansSR, digits=3)

RE.A.meansD <- RE.A.means[2,2]
round(RE.A.meansD, digits=3)

RE.A.meansO <- RE.A.means[3,2]
round(RE.A.meansO, digits=3)

#Making subsets of the spines

```

```

SpiderSR<-subset(Spider, Spine=="SoftRay")
SpiderSR
SpiderD<-subset(Spider, Spine=="Dorsal")
SpiderD
SpiderO<-subset(Spider, Spine=="Opercular")
SpiderO

SpiderF <- subset(Spider, Sex=="Female")
SpiderF
SpiderM <- subset(Spider, Sex=="Male")
SpiderM

SpiderFSR <- subset(SpiderF, Spine=="SoftRay")
SpiderFSR
SpiderFD <- subset(SpiderF, Spine=="Dorsal")
SpiderFD
SpiderFO <- subset(SpiderF, Spine=="Opercular")
SpiderFO

SpiderMSR <- subset(SpiderM, Spine=="SoftRay")
SpiderMSR
SpiderMD <- subset(SpiderM, Spine=="Dorsal")
SpiderMD
SpiderMO <- subset(SpiderM, Spine=="Opercular")
SpiderMO
#####

#t-test

ttest1 <- t.test(SpiderSR$RE.A, SpiderD$RE.A)
ttest1

ttest2 <- t.test(SpiderSR$RE.A, SpiderO$RE.A)
ttest2

ttest3 <- t.test(SpiderSR$RE.B, SpiderD$RE.B)
ttest3

ttest4 <- t.test(SpiderSR$RE.B, SpiderO$RE.B)
ttest4

```

```
#####
#####
plotLimitsREB<-as.data.frame(
  cbind(
    (RE.B.means[,2]+RE.B.sd[,2]),
    (RE.B.means[,2]-RE.B.sd[,2])
  )
)
colnames(plotLimitsREB)<-c("upper", "lower")
plotLimitsREB
###
plotLimitsREA<-as.data.frame(
  cbind(
    (RE.A.means[,2]+RE.A.sd[,2]),
    (RE.A.means[,2]-RE.A.sd[,2])
  )
)
colnames(plotLimitsREA)<-c("upper", "lower")
plotLimitsREA

#####

#####
#new improvement to the graph REB
windowsFonts(Calibri = windowsFont("Calibri"))
windows(6,5)
par(lwd=2, mar=c(5,5,1,1), family = "Calibri")

RE.Bplot<-barplot2(
  RE.B.means$RE.B,      #y values
  names.arg=RE.B.means$Spine, #x values
  plot.ci=TRUE,        #plot error bars?
  ci.u=plotLimitsREB$upper, #upper limit of error bars
  ci.l=plotLimitsREB$lower, #lower limit of error bars
  col=c("rosybrown","steelblue", "steelblue"),
  xlab=expression(italic("Spines")),
  ylab=expression(italic("Regulation RE.B")*(fold change)'),
  ylim=c(0, 1.1*round(max(plotLimitsREB$upper,2))),
  lwd=2,
  ci.lwd="2",
```

```

ci.width=0.4,
cex.lab = 1.2,
cex.axis=1
)
#Further graphical elements must be added AFTER 'barplot2'
abline(h=0, lwd=4)

#####
statsRE.B.O<-c(
  "",
  # "p = n.s.",
  paste0("p = ", zapsmall(tttest4$p.value, 2))
)

text(
  RE.Bplot[3,1],
  plotLimitsREB$upper+0.1*max(plotLimitsREB$upper),
  statsRE.B.O
)
#####
statsRE.B.D<-c(
  "",
  "p = n.s.",
  paste0("p = ", zapsmall(tttest3$p.value, 2))
)

text(
  RE.Bplot[2,1],
  plotLimitsREB$upper+0.1*max(plotLimitsREB$upper),
  statsRE.B.D
)

##We can save the plot as a high-resolution TIFF file (600 dpi) with "dev.print".
##Otherwise we can just copy or save the plot from the device window as METAFILE or other convenient
format..

dev.print(tiff,
  "RE.Bplot.tif",
  width = 12,
  height = 10,
  units = 'cm',

```

```

    type="windows",
    res=600
)

#####33
#REA GRAPH
windowsFonts(Calibri = windowsFont("Calibri"))
windows(6,5)
par(lwd=2, mar=c(5,5,1,1), family = "Calibri")

RE.Aplot<-barplot2(
  RE.A.means$REA,      #y values
  names.arg=RE.A.means$Spine, #x values
  plot.ci=TRUE,       #plot error bars?
  ci.u=plotLimitsREA$upper, #upper limit of error bars
  ci.l=plotLimitsREA$lower, #lower limit of error bars
  col=c("rosybrown","steelblue", "steelblue"),
  xlab=expression(italic("Spines")),
  ylab=expression(italic("Regulation RE.A")*(fold change)'),
  ylim=c(0, 1.1*round(max(plotLimitsREA$upper,2))),
  lwd=2,
  ci.lwd="2",
  ci.width=0.4,
  cex.lab = 1.2,
  cex.axis=1
)
#Further graphical elements must be added AFTER 'barplot2'
abline(h=0, lwd=4)

#####
statsRE.A.O<-c(
  "",
  "p = n.s.",
  paste0("p = ", zapsmall(ttest2$p.value, 2))
)

text(
  RE.Aplot[3,1],
  plotLimitsREA$upper+0.1*max(plotLimitsREA$upper),
  statsRE.A.O
)

```

```

dev.print(tiff,
  "RE.Aplot.tif",
  width = 12,
  height = 10,
  units = 'cm',
  type="windows",
  res=600
)

#####

statsRE.A.D<-c(
  "",
  "p = n.s.",
  paste0("p = ", zapsmall(ttest1$p.value, 2))
)

text(
  RE.Aplot[2,1],
  plotLimitsREA$upper+0.1*max(plotLimitsREA$upper),
  statsRE.A.D
)

#####3

dev.print(tiff,
  "RE.Bplot.tif",
  width = 12,
  height = 10,
  units = 'cm',
  type="windows",
  res=600
)

#####
#####
#####
#Homogeneity of Variances:

SpiderNew <- cbind(as.factor(paste0(Spider$Spine, Spider$Sex)),Spider)
View(SpiderNew)
colnames(SpiderNew)[1]<-"Condition"

```

```
leveneTest(data=SpiderNew, RE.A~Condition, center=median)
```

```
leveneTest(data=SpiderNew, RE.B~Condition, center=median)
```

```
#####
```

```
##SHAPIRO#Normality:#####
```

```
SRfem <- subset(SpiderNew, Condition=="SoftRayFemale")
```

```
SRfem
```

```
shapiro.test(SRfem$RE.A)
```

```
shapiro.test(SRfem$RE.B)
```

```
SRmas <- subset(SpiderNew, Condition=="SoftRayMale")
```

```
SRmas
```

```
shapiro.test(SRmas$RE.A)
```

```
shapiro.test(SRmas$RE.B)
```

```
#####
```

```
Dfem <- subset(SpiderNew, Condition=="DorsalFemale")
```

```
Dfem
```

```
shapiro.test(Dfem$RE.A)
```

```
shapiro.test(Dfem$RE.B)
```

```
Dmas <- subset(SpiderNew, Condition=="DorsalMale")
```

```
Dmas
```

```
shapiro.test(Dmas$RE.A)
```

```
shapiro.test(Dmas$RE.B)
```

```
#####
```

```
Ofem <- subset(SpiderNew, Condition=="OpercularFemale")
```

```
Ofem
```

```
shapiro.test(Ofem$RE.A)
```

```
shapiro.test(Ofem$RE.B)
```

```
Omas <- subset(SpiderNew, Condition=="OpercularMale")
```

```
Omas
```

```
shapiro.test(Omas$RE.A)
```

```
shapiro.test(Omas$RE.B)
```

```
#####

#####

SpiderAOVA <- aov(data=SpiderNew, RE.A~Spine*Sex)
summary(SpiderAOVA)

SpiderAOVB <- aov(data=SpiderNew, RE.B~Spine*Sex)
summary(SpiderAOVB)

tukeySPIDERa <- TukeyHSD(SpiderAOVA)
tukeySPIDERa

tukeySPIDERb <- TukeyHSD(SpiderAOVB)
tukeySPIDERb
#####
#
#####
#

SpiderRE.A = Spider[Spider$Sex %in% c("Male"),-c(1,3,4,5,6,8)]
SpiderRE.A

SpiderRE.AFem = Spider[Spider$Sex %in% c("Female"),-c(1,3,4,5,6,8)]
SpiderRE.AFem

SpiderRE.A <- cbind(SpiderRE.A, RE.AFem = SpiderRE.AFem[,2])
SpiderRE.A

meanA <- aggregate(. ~ Spine, SpiderRE.A, mean)
meanA

sdA <- aggregate(. ~ Spine, SpiderRE.A, sd)
sdA

plotmeanA <- rbind( meanA$RE.A, meanA$RE.AFem)

rownames(plotmeanA) <- c("Male", "Female")
colnames(plotmeanA) <- c("Dorsal", "Opercular", "SoftRay")
plotmeanA <- plotmeanA[, c(3,1,2)]
plotmeanA
```

```

plotsdA <-rbind( sdA$REA, sdA$RE.AFem)

rownames(plotsdA)<-c("Male", "Female")
colnames(plotsdA)<-c("Dorsal","Opercular", "SoftRay")
plotsdA<-plotsdA[, c(3,1,2)]
plotsdA

plotLimitsREA <-as.data.frame(cbind((meanA[,c(2,3)]+sdA[,c(2,3)]),(meanA[,c(2,3)] - sdA[,c(2,3)])) )
colnames(plotLimitsREA)<-c("upper", "upper", "lower", "lower")
plotLimitsREA

upperLimitsREA <-c(1.1*round(max(plotLimitsREA$upper,2)))

windowsFonts(Calibri = windowsFont("Calibri"))
windows(6,5)
par(mar=c(5,5,1,1), family = "Calibri", lwd=2)
dataPlot<-barplot2(plotmeanA,
  beside=TRUE,
  legend=TRUE,
  plot.ci=TRUE,
  ci.lwd = 2,
  ci.u=plotmeanA+plotsdA,
  ci.l=plotmeanA,
  col=c("steelblue","rosybrown"),
  lwd=2,
  ylab="Tx A: Relative Ef1a expression",
  ylim=c(0, 1.1*round(max(plotLimitsREA$upper,2))),
  xlab="Spines"
)
abline(h=0, lwd=2)
text( dataPlot,
  plotmeanA+plotsdA+max(4),
  cex=0.8
)

dev.print(tiff,
  "REAPLOT.tif",
  width = 15,
  height = 10,

```

```

units = 'cm',
type="windows",
res=600
)

#####
##
SpiderRE.B = Spider[Spider$Sex %in% c("Male"),-c(1,3,4,5,6,7)]
SpiderRE.B

SpiderRE.BFem = Spider[Spider$Sex %in% c("Female"),-c(1,3,4,5,6,7)]
SpiderRE.BFem

SpiderRE.B <- cbind(SpiderRE.B, RE.BFem = SpiderRE.BFem[,2])
SpiderRE.B

meanB <- aggregate(. ~ Spine, SpiderRE.B, mean)
meanB

sdB <- aggregate(. ~ Spine, SpiderRE.B, sd)
sdB

plotmeanB<-rbind( meanB$RE.B, meanB$RE.BFem)

rownames(plotmeanB)<-c("Male", "Female")
colnames(plotmeanB)<-c( "Dorsal","Opercular", "SoftRay")
plotmeanB<-plotmeanB[, c(3,1,2)]
plotmeanB

plotsdB <-rbind( sdB$RE.B, sdB$RE.BFem)

rownames(plotsdB)<-c("Male", "Female")
colnames(plotsdB)<-c( "Dorsal","Opercular", "SoftRay")
plotsdB<-plotsdB[, c(3,1,2)]
plotsdB

plotLimitsREB<-as.data.frame(cbind((meanB[,c(2,3)]+sdB[,c(2,3)]),(meanB[,c(2,3)]- sdB[,c(2,3)])) )
colnames(plotLimitsREB)<-c("upper","upper","lower","lower")
plotLimitsREB

```

```

upperLimitsREB<-c(1.1*round(max(plotLimitsREB$upper,2)))

windowsFonts(Calibri = windowsFont("Calibri"))
windows(6,5)
par(mar=c(5,5,1,1), family = "Calibri", lwd=2)
dataPlot<-barplot2(plotmeanB,
  beside=TRUE,
  legend=TRUE,
  plot.ci=TRUE,
  ci.lwd = 2,
  ci.u=plotmeanB+plotsdB,
  ci.l=plotmeanB,
  col=c("steelblue","rosybrown"),
  lwd=2,
  ylab="Tx B: Relative Ef1a expression",
  ylim=c(0, 1.1*round(max(plotLimitsREB$upper,2))),
  xlab="Spines"
)
abline(h=0, lwd=2)
text( dataPlot,
  plotmeanB+plotsdB+max(4),
  cex=0.8
)

dev.print(tiff,
  "REBPLOT.tif",
  width = 15,
  height = 10,
  units = 'cm',
  type="windows",
  res=600
)

```

A.4 Tx-B consensus sequence

>*Echiichthys vipera* Tx-B PARTIAL 815bp

```
TGTTGGAGTTCATGTCTTCAGAAATCTTGGTGGCAGCTGCCTTGGGTTCGACCATTAC-  
CTTAGGGGCGTTGTATGATGCCAGGCAAGATAAACTGATCCCAGGTTTCACATTGTGGGATGAAG  
AGGTTCTGAAGGACTCCACATTTGAAAGCCCTCTGCCAGCAGTGCATTT-  
GAAATCATAGCGTCTGATGCCATCGATGACAAGTCTAATCTGCTGGATGTTGAAGCTTCTCTCAA  
GCCAGTTTCCTGGGTGGACTGGTGGGAAGTCGGAGGATCTGCCAAGTATCTGAATAATACGAA-  
GAAATTCAAGAATCAGAGTCGAGTGACACTTCAGTACAAAGCTACCACAACCTTCAAACAGTTGAT  
GACTCACCTTGGAAGCAAGCATGTAGAATATTCTGAATTATTCGAGAGCATCAAA-  
GCAACTCATGTAGTGATAGGGATCCTTTATGGGGCCAATGCTTTCTTCGTCTTTGACAGTGACAA  
AGTAGATTCTAGCAACGTTTCAGGATATTCAGGGCAGCATGGAAGCTGTGATAAAGAA-  
GATCCCCTCGGTGGAAATCTCAGGTCGAGGTGCCGTCCAGCTAACCAGTGAAGAAAGTGACATA  
ACCAACAACCTTCACCTGCAAATTCACGGGGACTTCGTTCTCACAAGTAATCCAAC-  
GACTTTTCAGGATGCAGTTCAAACCTTACCAGAACTTCCACAGATGACGAGCAAAGACGCTTCTG  
TTCCAATGACGGTCTGGCTCGTGCCGCTGACGAGTTTTTACTCTAAAGCACCTCAGCTG-  
GATGCTGATAGCAGCACTCCAATACTT
```




<2024>

SAMUEL RAMOS PEREIRA

VARIATION OF VENOM COMPOSITION AND TOXICITY IN WEEVER FISHES (TRACHINIDAE).
IMPLICATIONS FOR BIOMEDICINE AND BIOTECHNOLOGY